TUDelft

Delft University of Technology

Field experiments at three sites to investigate the effects of age on steel piles driven in sand

Carroll, R.; Carotenuto, P.; Dano, C.; Salama, I.; Silva, M.; Rimoy, S.; Gavin, K.; Jardine, R.

Important note
To cite this publication, please use the final published version (if applicable).
Please check the document version above.

Field experiments at three sites to investigate the effects of age on steel piles driven in sand

R. CARROLL*, P. CAROTENUTO†, C. DANO‡, I. SALAMA‡, M. SILVA§, S. RIMOY‖, K. GAVIN¶ and R. JARDINE**

This paper investigates the influences that steel type, in situ soil properties, water table depth, pile diameter, roughness and driving procedures have on the ageing behaviour of piles driven in sand. Tension tests have been performed on 51 open-ended steel micro-piles, with 48 to 60 mm outside diameter, driven at well-established research sites at Larvik in Norway, Dunkirk in France and Blessington in Ireland to better understand the processes that control axial capacity set-up trends in the field. Mild steel, stainless and galvanised steel micro-piles were driven and left to age undisturbed for periods of between 2 h and 696 days before being subjected to first-time axial tension load tests. In addition to reporting and interpreting these experiments, further investigations of the sites' geotechnical profiles are reported, including new piezocone and seismic cone penetration soundings as well as laboratory tests. Integration with earlier ageing studies at the same sites with larger (340 to 508 mm outside diameter) open-ended steel piles driven to 7 to 20 m embedments and experiments that varied the piles' initial surface roughness shows that corrosion, pile scale, roughness, the bonding of soil particles and the driving process can all be highly significant. New insights are gained into the mechanisms that control the axial capacity of piles driven in sand.

KEYWORDS: model tests; offshore engineering; piles & piling; sands; time dependence

INTRODUCTION

Studies of the reliability of conventional design methods (including the internationally applied API (2011) main text method) predictions for the axial capacities of large piles driven in sands have revealed wide scatter and significant bias; see, for example, Tang *et al.* (1990) or Jardine & Chow (1996). Alternative methods that offer better reliability include the Fugro-05 (Kolk *et al.*, 2005), ICP-05 (Jardine *et al.*, 2005), NGI-05 (Clausen *et al.*, 2005) and UWA-05 (Lehane *et al.*, 2005) approaches. All four, which are now cited in API's commentary, employ site-specific CPT profiling to characterise the sand state and recognise the effect of the relative pile tip depth (h) on shaft capacity. Independent database studies by Yang *et al.* (2017) and Lehane *et al.* (2017) involving high-quality load tests on piles with outside diameters exceeding 0·2 m gave broadly similar results, showing that the 'full' ICP-05 and UWA-05 methods for sands offer the lowest degrees of predictive scatter and bias. Field pile driving monitoring has also confirmed that 'full' ICP-05 predictions are representative of the shaft capacities

developed by large offshore piles within a few days of driving; see Overy (2007) or Jardine *et al.* (2015).

However, most field load tests are conducted relatively soon after driving and axial capacities change with time. Schmertmann (1991), Åstedt *et al.* (1992), Chow *et al.* (1998), Bea *et al.* (1999), Axelsson (2000), Jardine *et al.* (2006), Gavin *et al.* (2013), Karlsrud *et al.* (2014), Lim & Lehane (2014), Gavin *et al.* (2015) and Rimoy *et al.* (2015), among others, have reported marked growth over weeks and months after driving in sands, although the data are often widely scattered and the processes that control ageing remain uncertain. Ageing appears to benefit shaft capacity primarily (Rimoy *et al.*, 2015) and its effects are clearest in 'first-time' tension tests to failure. Jardine *et al.* (2006), Karlsrud *et al.* (2014), Rimoy *et al.* (2015) and Gavin *et al.* (2015) reported from 'first-time' tension tests on open-ended steel piles (340 mm < OD < 508 mm (OD, outside diameter)) at three sand sites the systematic trend shown in Fig. 1. Capacity growth took place in the first 8 months after installation before reaching an upper limiting capacity, around 2·5 times higher than the ICP-05 predictions. The ICP-05 capacities were exceeded within 2 weeks of driving.

Rimoy & Jardine (2015) and Rimoy *et al.* (2015) collated ageing data from tests on 103 industrial (0·2 < OD < 1·3 m) piles conducted at various ages after driving in sand, as summarised in the Appendix. Most involved multiple re-tests on individual piles after relatively short pauses, so promoting scatter and systematically slower capacity growth trends than are seen in first-time tests (Jardine *et al.*, 2006). The compression capacities include base capacity components that may be of similar, or greater, magnitude to the shaft resistances and may grow as ever larger tip settlements accumulate through re-testing. These factors and a lack of cone penetration test (CPT) and other site information make the trends harder to interpret than the research outcomes presented in Fig. 1. However, the scatter diagrams presented in Figs 2(a) and 2(b) from datasets of compression tests in Rimoy *et al.* (2015) indicate similar overall set-up trends for
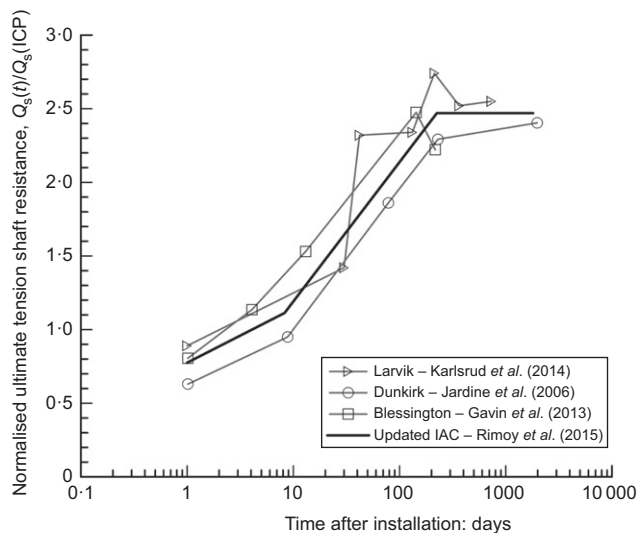
Fig. 1. Static tension capacity–time trends from first-time tests on steel piles driven at three sand sites, normalised by ICP-05 tension capacities. IAC refers to intact ageing characteristic, as defined by Rimoy et al. (2015)
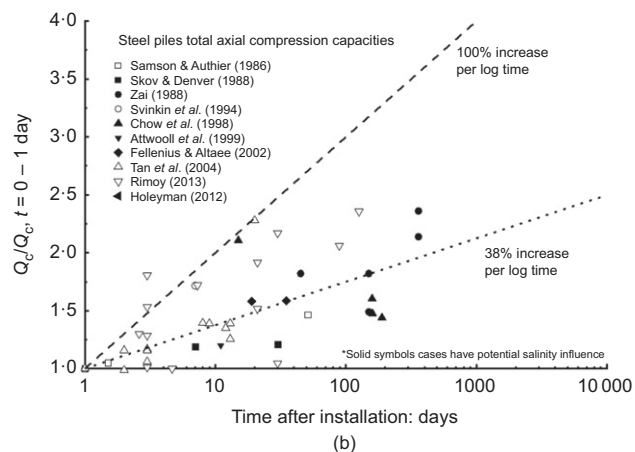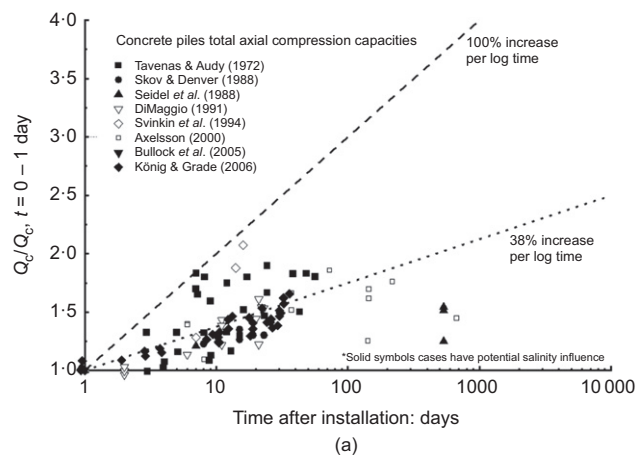

Fig. 2. (a) Concrete driven piles' total axial compression capacities. (b) Steel driven piles' total axial compression capacities

concrete and steel piles. Rimoy et al. (2015) also note that groundwater salinity did not appear to be a key factor, and that wooden piles set-up in sands and hard driving reduces short-term axial capacity and provides scope for more marked set-up after installation.

Chow et al. (1998) proposed three mechanisms to explain the effects of age on shaft capacity

(a) stress redistribution leading to higher stationary radial effective stresses σ'_{rc} acting on the shafts
(b) gains under axial loading of the dilative shaft radial stress $\Delta\sigma'_{rd}$ capacity component, as demonstrated in instrumented field tests by Lehane et al. (1993) and Chow (1997)
(c) physicochemical processes involving the soil and shaft.

Gavin et al. (2013) noted that stress redistribution after driving caused the radial effective stress on their instrumented pile to reduce with time. They concluded that the primary mechanism contributing to the ageing of their 340 mm OD steel piles was increased dilative response with time (mechanism (b)). A secondary effect involved sand particles bonding to the lower pile shaft, leading to changes in shaft roughness and migration of the shear failure surface into the sand mass (mechanism (c)). In contrast Chow et al. (1998) and Jardine et al. (2006) noted the importance of increases in radial effective stresses acting on the pile shaft (mechanism (a)) to gains in pile capacity.

Jardine & Standing (2012) reported further that low-level cyclic loading enhances capacity. White & Zhao (2006) investigated the impact of environmental or seasonal cycles on pile ageing. They report that the set-up rates of model mild steel piles increased when water depth was cycled, although stainless steel piles showed no gains with time. Other work suggests that the installation process might also be significant. Lim & Lehane (2014) noted considerably less set-up and 'friction fatigue' with small-diameter jacked piles than with piles driven at the same site and argued that ageing involves a recovery process that leads to a stable final upper-bound outcome, as seen in the tests summarised in Fig. 1.

Rimoy et al. (2015) report intensive long-term calibration chamber testing on 36 mm OD, closed-ended, jacked and driven piles in medium-dense silica sand. Their experiments aimed to study the ageing process under closely controlled conditions and included comprehensive measurement of the normal stresses developed on pile shafts and in the sand mass. However, the model piles developed far less set-up than the industrial piles reported in Figs 1 and 2. Imposed cycles of environmental stress change also had little influence on pile capacity.

Tsuha et al. (2012) found that low-level cyclic axial loading improved the same model piles' tension capacities, whereas high-level cycling or hard driving severely damaged capacity, as with industrial piles (Jardine & Standing, 2012). Rimoy et al. (2015) suggested that interrelated cyclic and ageing stress re-distribution mechanisms exist that are affected by the bands of fractured and compacted sand that form around steel displacement piles when $q_c > 8$ MPa. Yang et al. (2010) found bands of adhered sand ≈ 5 to $20D_{50}$ thick around their 36 mm model piles whose width grew with relative tip depth, h, and amounted to 0·5 to 1·5 mm, averaging around $D/30$. Rimoy et al. (2015) argue that the arching mechanism on the outer pile wall may be affected by the ratio of D/D_{50} and that the stress re-distribution mechanism may not apply as effectively to small-diameter closed-ended piles.

Growth of either shaft roughness or sand stiffness with age could increase the dilatant $\Delta\sigma'_{rd}$ component of shaft capacity that is captured by the ICP-05 design approach and varies (as proposed by Boulon & Foray (1986)) with $1/D$. Outward radial expansion of the shaft through corrosion reactions could also raise σ'_{rc} while cementing of the fractured sand zone by iron compounds could increase the constant volume interface friction angles, δ_{cv}, and could lead, ultimately, to

Table 1. Meteorological data published for the locations nearest the three sites

Site	Rainfall (annual): mm	Temperature Monthly averages		Humidity Monthly averages	
		Min.: °C	Max.: °C	Min.: %	Max.: %
Blessington (Dublin, Ireland)	734	5	16	73	83
Dunkirk (France)	710	4	18	78	84
Larvik (Norway)	763	2	16	60	85

soil–soil shear strength controlling the long-term shaft resistance.

This paper reports experiments with 51 micro-piles ($48 < D < 60$ mm) driven and tested statically at various ages in tension at the Larvik (Norway), Dunkirk (France) and Blessington (Ireland) sites where the earlier experiments summarised in Fig. 1 were conducted. Mild (MS), stainless (SS) and galvanised (GS) steel piles were driven above and below the water table under the broadly similar climatic conditions outlined in Table 1. Some piles were installed with smooth and un-corroded surfaces, while others were pre-corroded or pre-driven to modify their surfaces. The experiments investigated how pile material, roughness and diameter affected ageing at three well-characterised research sites with different sand profiles. The piles were left undisturbed during the ageing period. Daily to seasonal temperature changes and possibly pore water suction fluctuations above the water table at Dunkirk and at Blessington were the only environmental variations experienced over the ageing periods. The central questions investigated are listed below.

(a) How influential to ageing are any physicochemical processes associated with the pile material, the soil and groundwater?
(b) Do other pile-specific factors such as scale, shaft roughness, installation process or environmental site conditions affect the outcomes?
(c) Does any upper shaft capacity limit, such as $\approx 2 \cdot 5$ times the ICP-05 medium-term prediction apply, as indicated by Fig. 1, irrespective of any continuing active ageing processes?

DESCRIPTION OF TEST SITES

Karlsrud *et al.* (2014) established the Norfolk Geotechnical Institute's (NGI's) test site, in the Larvik municipality (Norway) around 110 km southwest of Oslo, in the Numedalslågen estuary, which has a small tidal range. The ground surface is $2 \cdot 4$ m above sea level; 2 m of made ground overlies loose-to-medium-dense fluvial silty sands and silt layers down to at least 22 m. The grain size distributions applying over the study depth range indicate 5 to 20% silt, as presented in Fig. 3. Radiocarbon dating indicates deposition 2600 to 1200 before present (bp), while X-ray diffraction (XRD) testing on a $7 \cdot 9$ m deep sample indicates 25% quartz, 37% feldspars and 38% plagioclase and no clay minerals (NGI, 2009).

Nine CPT tests within the 15 m by 30 m test area showed piezocone $q_{c\text{-min}}$ and $q_{c\text{-avg}}$ consistently around 1 and $2 \cdot 1$ MPa, respectively, over the $3 \cdot 5$ to 7 m depth range, while $q_{c\text{-max}}$ showed greater variation ($2 \cdot 8$ to $5 \cdot 5$ MPa); see Figs 4(a) and 5. Piezocone excess pore pressures measured at the u_2 position were generally positive and often around 30 kPa (and in some cases 120 kPa); see Fig. 4(d). Samples from the boreholes identified in Fig. 5 showed the profile
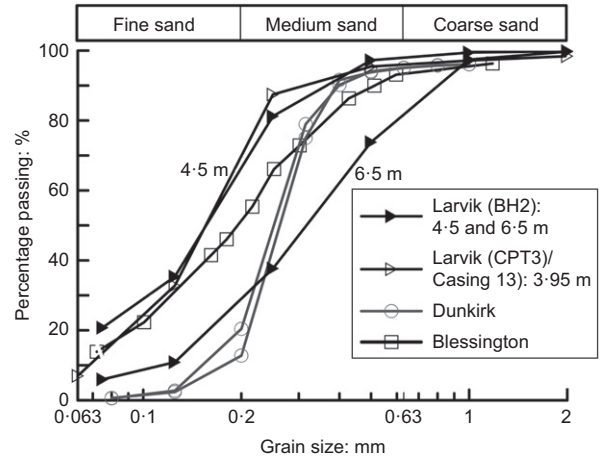
Fig. 3. Grain size distribution for Larvik, Dunkirk and Blessington

becoming siltier at depth; the CPTu results over 20 m depth led Lehane *et al.* (2017) to exclude the larger Larvik piles from their database of tests in free-draining silica sands. Ring shear interface and triaxial tests run at Imperial College on borehole samples gave the mechanical parameters listed in Table 2, while the chemical testing results in Table 3 indicate acidic groundwater conditions.

The Dunkirk Port-Ouest site described by Jardine *et al.* (2006), near Gravelines, Northern France, consists of dense-to-very-dense marine sand under hydraulic fill derived from the marine sand. The PISA project (Byrne *et al.*, 2015) provided a 25 by 15 m area in which 50 mm dia. micro-piles were driven to ≈ 2 m, 2–3 m above the water table, within the hydraulic fill; see Fig. 6. The test locations were not affected by sea tides. Grain size distributions are shown in Fig. 3; other soil mechanical parameters are summarised in Table 2 and chemical testing is reported in Table 3. The sub-angular particles comprise $\approx 85\%$ silica plus calcium carbonate ($CaCO_3$) shell fragments and other minerals that leave the soil slightly alkaline (Chow, 1997). Ring shear interface and triaxial tests run at Imperial College gave the mechanical parameters listed in Table 2; higher ϕ'_p can be expected at $D_r = 100\%$ (see Kuwano (1999)). CPT and seismic CPT test investigations performed for the PISA project (Zdravković *et al.*, 2019) and this ageing study provided the representative CPT profiles plotted in Fig. 4(b). CPT tests 01, 03 and 04, show q_c increasing from zero to up to 40 MPa at $1 \cdot 5$ m depth before reducing significantly. The 19 Panda2® dynamic penetrometer tests conducted as shown in Fig. 6 are not reported in detail but indicated denser conditions in the central test area. Emerson *et al.* (2008) noted that a surface failure mechanism affects the tip resistances developed in shallow CPT tests until a critical depth z_{crit} is exceeded. They propose an expression for z_{crit} that involves CPT diameter, tip resistance and sand unit weight which indicates that near-surface effects probably
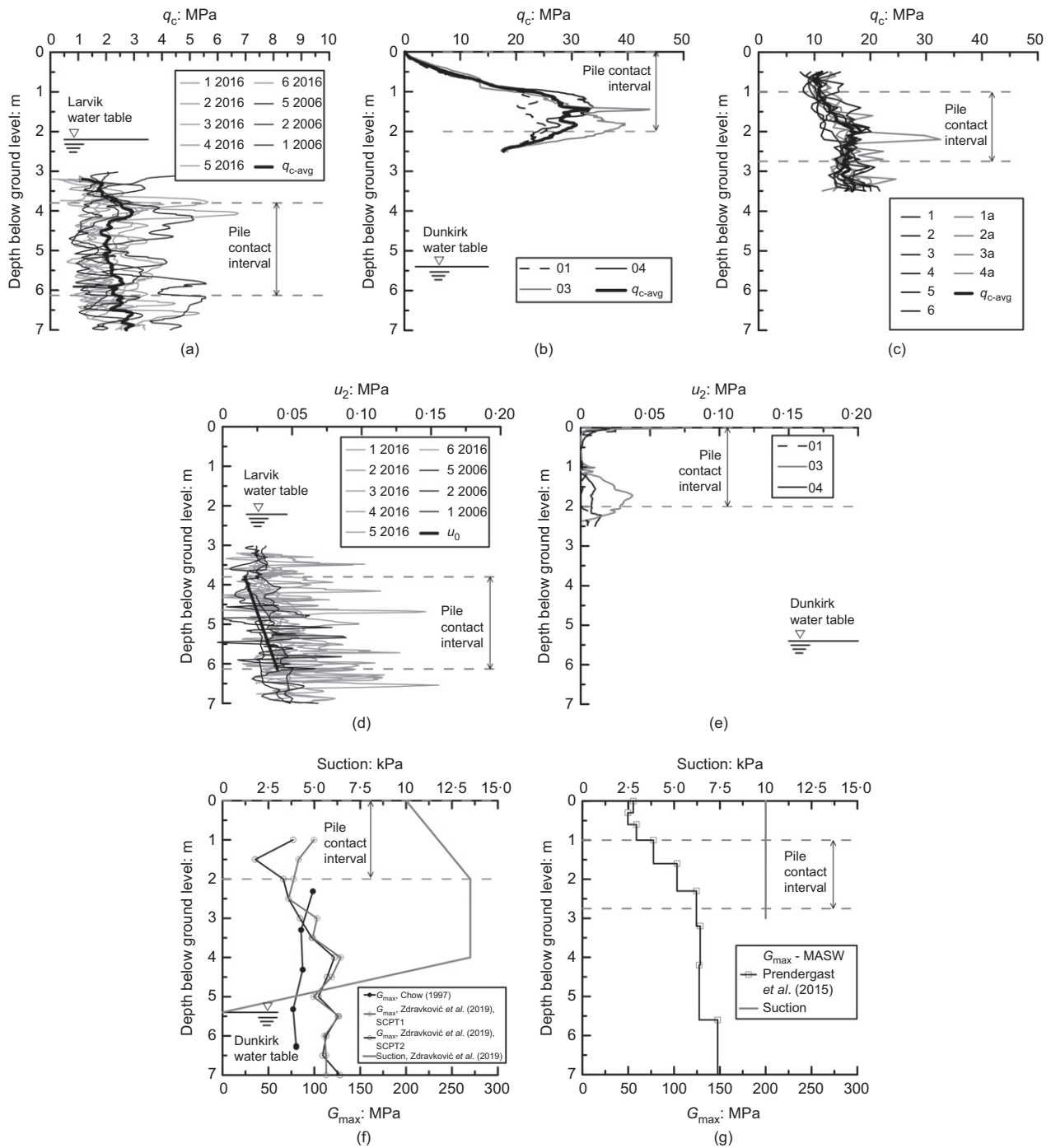
Fig. 4. (a) q_c variation with depth at Larvik, '2016' refers to CPT performed in 2016 and '2006' refers to CPT performed in 2006 by Karlsrud *et al.* (2014), see also Fig. 5; (b) q_c variation with depth at Dunkirk; (c) q_c variation with depth at Blessington; (d) u_2 variation with depth at Larvik, '2016' refers to CPT performed in 2016 and '2006' refers to CPT performed in 2006, see also Fig. 5; (e) u_2 variation with depth at Dunkirk; (f) suction and G_{max} variation with depth at Dunkirk; (g) suction and G_{max} variation with depth at Blessington

reduced the q_c values down to 1·5 m depth at Dunkirk. Shallower z_{crit} depths are indicated for Larvik, which do not affect the CPT profiles applying over the Larvik test piles' 3·8 to 6·2 m contact depth range.

The seismic CPT traces plotted on Fig. 4(f) indicate relatively high G_{max} values. Piezocone soundings conducted adjacent to the micro-pile indicated u_2 pore pressures that were generally zero or negative (down to −15 kPa) over the depth range of interest, although positive pressures of up to 40 kPa were seen over intervals where fines contents were higher; see Fig. 4(e). Suctions of ≈10 kPa that may have varied seasonally were found in 'hanging water' laboratory measurements (see Dane & Hopmans (2002)) on block

samples taken in winter adjacent to the piles. The suction profile interpreted for the PISA programme and shown on Fig. 4(f) was taken as representative in the analyses that follow.

The Blessington site is located 25 km southwest of Dublin city. As documented by Gavin & O'Kelly (2007), Gavin *et al.* (2009) and Doherty *et al.* (2012), glacial deposition coupled with recent quarrying has left the test location in an overconsolidated state. The water table is ≈13 m deep and ground conditions comprise very dense ($D_r ≈ 100\%$) glacially deposited medium-to-fine sand composed of quartz and hard limestone ($CaCO_3$) grains which impart alkalinity to the sand. Fig. 3 shows the sand's average grading curve; other
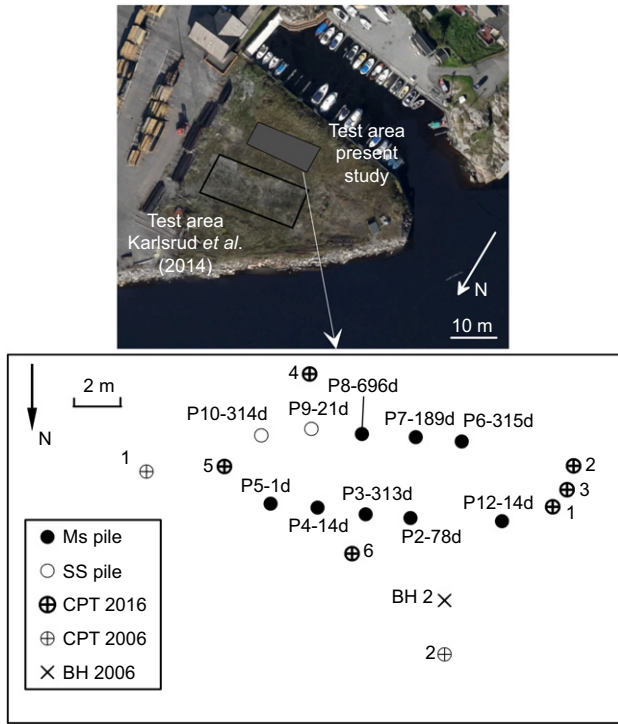
Fig. 5. Larvik site layout

mechanical soil properties are summarised in Table 2 while Table 3 provides chemical test results. The pile layout is shown in Fig. 7. Eight CPT tests performed within 5 m of the micro-piles (Prendergast *et al.*, 2015) showed average q_c increasing from 10 MPa to 15 MPa at 3 m, see Fig. 4(c). The Blessington test piles were driven from 1 m deep starter holes and the Emerson *et al.* (2008) analysis indicates that the CPT profiles should be mainly free of any shallow-penetration effects. Given the 13 m water table depth, piezocone tests were not undertaken. Water contents are $\approx 11\%$ over the first 2 m, where 10 to 12 kPa suctions were measured in situ with Decagon T4 tensiometers with filter lengths between 0·30 m and 1·15 m. The suctions may vary seasonally, but there are no other significant environmental cyclic actions to consider. Fig. 4(g) displays the G_{max} profile interpreted from multi-channel analysis of surface waves (MASW) reported by Prendergast *et al.* (2015) and the interpreted in situ suctions.

EXPERIMENTAL PROGRAMME
Piles and installation

Details of the micro-piles tested in this study are summarised in Table 4, while Tables 5–7 report the details of plug formation at the end of pile installation as the final plug length ratios (PLRs), defined as the internal plug length divided by the pile embedment depth.

Seven 50 mm OD mild steel (MS) and two 48·2 mm OD stainless steel (SS) open-ended tubular piles were driven at Larvik to 6·2 m tip depth, well below the water table. The piles were driven through cased holes pre-bored to 3·8 m depth (see Fig. 5), giving an embedment length of 2·4 m.

Table 2. Summary of soil parameters and ground conditions for three test sites

	Unit	Larvik*	Dunkirk	Blessington
Water table BGL	m	2·2	5·4	13
Description		Loose to medium dense silty fine to medium sand with some silt layers	Dense to very dense sand	Dense, medium to fine sand
Origin		Fluvial	Marine hydraulic fill	Glacial
Unit weight (γ_{bulk})	kN/m³	18·9–19·6	17·1†	20·0‡
Water content	%	26·5	5–7	10‡
Relative density (D_r)	%	~20	100	100
Saturation (S_r)	%	100‡‡	25–40‡‡	60‡‡
D_{90}	mm	0·37–0·8	0·4	0·6
D_{50}	mm	0·16–0·38	0·26	0·1–0·15‡
Fines < 0·063 mm	%	6–20	0	5–10
Effective peak, ϕ'_p (triaxial) and test conditions	deg	36, $\sigma'_3 = 200$ kPa¶ $e_0 = 0·80$ $D_r = 45\%$ (estimated)	37, $\sigma'_3 = 200$ kPa** $e_0 = 0·64$ $D_r = 75\%$	42, $\sigma'_3 = 200$ kPa‖ $e_0 = 0·59$ $D_r = 100\%$ (estimated)
Constant volume, ϕ'_{cv} (triaxial)	deg	35, $\sigma'_3 = 200$ kPa¶	32, $\sigma'_3 = 200$ kPa**	35, $\sigma'_3 = 200$ kPa‖
Constant volume interface shear δ_{cv} and test conditions	deg	27·8, $\sigma'_n = 200$ kPa¶	27·5, $\sigma'_n = 200$ kPa¶	29·4, $\sigma'_n = 200$ kPa¶
Overconsolidation ratio (OCR)		1	1	15 at 1 m§ 5 at 5 m§
Average q_c	MPa	2	30	15‖
Average f_s	MPa	0·02	0·1–0·3	0·16‖
Small-strain stiffness value, G_{max}	MPa	—	50–130††	50–150‖

*NGI (2009).
†Chow *et al.* (1998) and Chow (1997).
‡Gavin & O'Kelly (2007).
§Doherty *et al.* (2012).
‖Prendergast *et al.* (2015).
¶2017–2018 triaxial and interface ring shear tests at Imperial College. Interface shear tests conducted against mild steel interfaces with R_{CLA} 8 to 13 µm, following Jardine *et al.* (2005) procedures.
**After Aghakouchak *et al.* (2015).
††Zdravković *et al.* (2019).
‡‡Nominal as S_r varies with time and depth.

Table 3. Chemical tests on sand samples from the three sites

	pH	Sulfate (SO_4): mg/kg TS	Carbonate (CO_3): % TS	Total inorganic carbon: % TS	Conductivity: mS/m
Dunkirk	8·6	1000	9·5	1·9	8·3
Larvik	3·5	11 900	0·1	0·02	67·7
Blessington	8·0	<1000	20·5	4·1	8·6

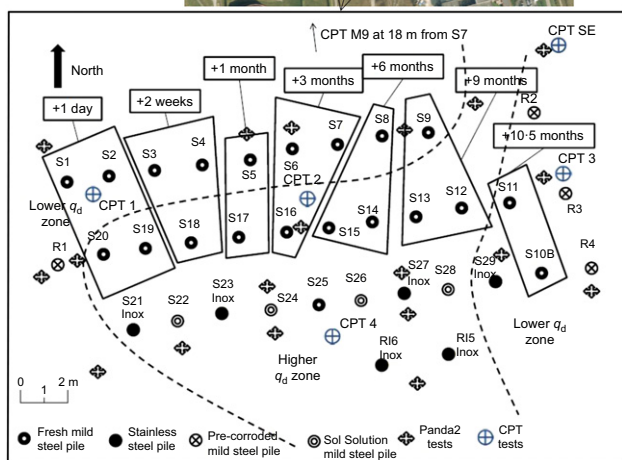Note: TS, total solids.

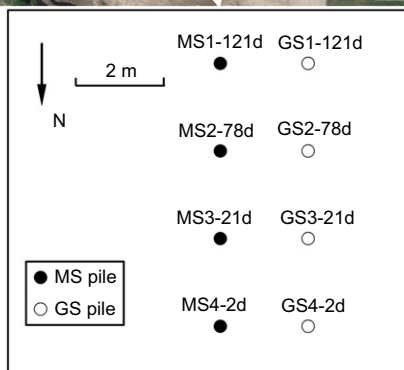**Fig. 6. Dunkirk site layout**

Fig. 7. Blessington site layout

Fig. 8, A.1 shows the visual condition of the Larvik piles prior to installation. The outsides of the SS piles were air-abraded, and the MS piles were deliberately pre-corroded by 4 months' exposure on site before driving (with the exception of pile 2, which was left exposed for some days). Check measurements on spare MS and SS piles that had been exposed for up to a year on site gave average R_{cla} roughness values of 8·5 and 9·8 μm, respectively, with a Mitutoyo Surftest-SJ-210-Series-178, that match the typical $R_{cla} \approx 10$ μm of industrial piles (Jardine *et al.*, 2005). The piles were installed by a 0·62 kN weight drop-hammer that could fall between 0·20 and 0·35 m and impart energies between 74 and 130 Joules/blow, assuming 60% efficiency. A removable temporary cage inserted in the cased holes ensured pile verticality during installation.

In total, 31 open-ended piles were driven at Dunkirk, as shown in Fig. 6, in the southeast corner of the PISA site, 20 m from the nearest PISA pile. Multiple roughness measurements with a portable Taylor Hobson Surtronic 25 indicated pre-installation $R_{cla} = 2 \pm 1$ μm for the 21 fresh MS piles (S1 to S20 and S25) and four stainless steel piles (S21, S23, S27 and S29-Inox) that were driven from ground level in January 2016. An adjustable Sol Solution Grizzly® machine was employed whose maximum energy (475 Joules/blow) and 60 to 70% energy ratio is equivalent to that of a standard penetration test (SPT) hammer. Four of the 21 MS piles were extracted after 4 months and re-driven as 'pre-corroded' rougher piles (R1, R2, R3 and R4). Their rougher shafts and sand adhering to their interiors led to lower PLRs than with fresh piles. Two of the four SS piles were extracted and air-abraded on their outsides before re-driving in July 2016 as RI5 and RI6. While R_{cla} values were measured before testing for most piles, this was not feasible for MS piles R1 to R4, as their R_{cla} values were higher than the Surtronic 25 could measure, as well as for SS piles R15 and R16. Visual inspection and tactile checks indicated R_{cla} values comparable to those of lightly rusted industrial piles (≈ 10 μm) for MS piles R1 to R4, while the re-driven shot-blasted SS piles were gauged to have been little affected by the air-abrasion applied and to have retained $R_{cla} \approx 2$ μm.

Driving took place in January 2016 at Blessington, with the four pairs of 60 mm OD, 4 mm thick MS and galvanised (GS) tube-piles shown in Fig. 7. The MS piles were mildly pre-corroded. The GS piles' manufacture involved molten zinc dipping, which left a moderately rough surface; R_{cla} values were estimated as ≈ 10 μm for both pile types. The top metre of sand was augered to avoid contact with superficial material. Handheld metal post drivers were employed until all piles effectively refused after penetrations of 0·5 to 0·7 m. Pile MS1 was damaged and had to be abandoned; a greatly over-sized 4 t hammer was employed the next day to achieve the final 2·75 m tip depths. Although the piles were not exhumed, earlier studies by Gavin *et al.* (2013) at Blessington indicate that crusts of crushed sand are likely to have formed around the shafts on driving that may have undergone chemical modification during ageing. The mild steel piles are likely to have corroded in situ.

Table 4. Properties of piles

		Larvik	Dunkirk	Blessington
R_{cla} fresh MS‡	µm	—	1–3§ ≈ 10 after extraction* †‖	—
R_{cla} pre-corroded MS	µm	NA§ 9·2‖ 8·5¶	≈ 10* § ≈ 10 after extraction * †‖	≈10* §
R_{cla} SS/GS	µm	—	1–3§ ≈ 1–3 after extraction* ‖	≈10* §
R_{cla} air-abraded SS	µm	NA§ 10·3‖ 9·8¶	≈ 1–3* § ≈ 1–3 after extraction* ‖	—
Grade MS	—	EN 10305-3 (BSI, 2016), E220 + CR2 – S2	E470	NA
Grade SS/GS	—	AISI 304	316L	NA
Outside diameter	mm	50-MS 48·2-SS	51-MS 50·6-SS	60
Wall thickness (t)	mm	2	8-MS 7·5-SS	4
D/t ratio	—	24–25	6·3–6·7	15
Contact length average	m	2·4	1·97	1·75

Note: MS, mild steel; SS, stainless steel; GS, galvanised steel; NA, not available.
*Estimated.
†Sand adhered to the pile.
‡The 'fresh' interfaces were as delivered to site without any deliberate pre-corrosion or further air abrasion.
§Measured centre-line average roughness (R_{cla}) prior to installation.
‖Measured centre-line average roughness (R_{cla}) as found on extraction post tension test, including any in situ corrosion.
¶Measured centre-line average roughness (R_{cla}) as found on spare not installed piles left exposed over 1 year on site.

Table 5. Peak pile capacities for Larvik

Pile ID	Time: days	Capacity: kN	Pile	Driving energy	Plug length ratio (PLR)
P05	1	2·60	MS*	Variable	0·29
P04	14	3·71	MS*	Variable	0·52
P12	14	4·26	MS*	Variable	0·32
P02	78	3·94	MS*	Variable	0·42
P07	189	4·74	MS*	Variable	0·43
P03	313	5·45	MS*	Variable	0·40
P06	315	5·96	MS*	Variable	0·42
P08	696	5·45	MS*	Variable	0·54
P09	21	2·66	SS†	Variable	0·60
P10	314	2·43	SS†	Variable	0·54

*Pre-corroded.
†Air-abraded. Failure defined at peak.

Testing arrangements

Equipment and procedures varied between sites. The Larvik piles' first-time static tension capacities were measured 1, 14, 21, 78, 189, 315 and 696 days after driving with the system shown in Fig. 9. An extension rod connected the pile head, through a load cell, to a suspended hydraulic cylinder actuated by a GDS ADVPC advanced pressure/volume controller. Jack pressures were raised gradually and held constant for 20 min over load stages. A SignalExpress logging system recorded time, load and vertical pile movements relative to the pre-installed casings, which were assumed unaffected by loading. Tests ended when clear load–displacement plateaux developed, and displacements exceeded 7 mm (14% of the piles' OD).

The Dunkirk piles were subject to static tension tests after 0·1, 1, 14, 28, 90, 175, 272 and 315 days' ageing. The reaction frame comprised four steel beams that transferred load to timber foundations; see Figs 10(a) and 10(b). An Enerpac manual hydraulic jack acted through a load cell. Load increments were set initially at 10% of the estimated medium-term tension capacity (that reduced as failure approached) and maintained for 15 min. Tests continued until displacements reached 15 to 30 mm (30 to 60% of pile OD) as measured by two linear variable differential transducers (LVDTs) supported on vertical stands set 0·7 m on either side of the pile axis (Fig. 10(a)). A third LVDT measured the loading system deformation and the corrected mean LVDT displacement was applied in test analysis. Strong winds affected displacement measurements in some tests.

The Blessington static load tension tests were carried out 2, 21 and 78 days after driving. The 121 day MS1 pile was abandoned and equipment malfunctioned in the 121 day GS pile test. Testing arrangements were similar to those at Dunkirk, see Fig. 11. Displacement measurements relied on a reference beam and three magnetically clamped LVDTs. An Enerpac manual hydraulic jack applied ≈ 5 kN load increments, while the LVDTs and the load cell outputs were recorded by a Campbell Scientific data logger at 0·1 s intervals and transferred to a computer. Load steps were held constant for 30 s and tests terminated when it was no longer possible to maintain loads by jacking. The final displacements exceeded 20 mm (33% of pile OD). Most tests ended within 10 min, while those at Larvik and Dunkirk extended several times longer.

FIELD BEHAVIOUR
Installation

The Larvik piles' driving drop-weight heights increased from 0·2 m to 0·35 m as penetration advanced, giving the blow-count envelopes and means in Fig. 12(a). The final PLRs ranged from 0·29 to 0·60, with SS piles showing slightly higher ratios than the pre-corroded MS piles; see Table 5.

At Dunkirk the Sol Solution 'Grizzly' machine drove piles S1 to S9 at its maximum (SPT) energy level. Lower ratings (from 21% up to 100%) were applied to other piles to achieve consistent penetration rates and Fig. 12(b) presents the

Table 6. Peak pile capacities for Dunkirk

Pile ID	Time: days	Capacity: kN	Pile	Driving energy	Plug length ratio (PLR)
S1	0·1	28·6	MS*	SPT	0·43
S2	2	29·7	MS*	SPT	0·52
S3	16	62·6	MS*	SPT	0·43
S4	16	59·3	MS*	SPT	0·36
S5	30	56·7	MS*	SPT	0·38
S6	92	67·4	MS*	SPT	0·41
S7+	93	64·2	MS*	SPT	0·41
S8	175	70·6	MS*	SPT	0·43
S9	274	71·1	MS*	SPT	0·38
S10B	315	71·7	MS*	Variable	0·46
S11	315	67·6	MS*	Variable	0·50
S12	273	79·6	MS*	Variable	0·49
S13+	273	76·7	MS*	Variable	0·40
S14+	176	73·9	MS*	Variable	0·48
S15	174	78·2	MS*	Variable	0·49
S16	90	71·6	MS*	Variable	0·40
S17	28	66·5	MS*	Variable	0·42
S18	14	67·8	MS*	Variable	0·43
S19	1	32·8	MS*	Variable	0·38
S20	0·1	31·2	MS*	Variable	0·36
R1	1	50·2	MS†§	Variable	0·22
R2	85	89·0	MS†§	Variable	0·21
R3	183	66·3	MS†§	Variable	0·24
R4	223	76·3	MS†§	Variable	0·23
S21-Inox	0·1	25·9	SS	Variable	0·38
S23-Inox	14	25·8	SS	Variable	0·44
S27-Inox	28	24·6	SS	Variable	0·43
S29-Inox	91	27·6	SS	Variable	0·44
RI5	1	32·3	SS‡§	Variable	0·38
RI6	99	25·6	SS‡§	Variable	0·38

*Fresh.
†Pre-corroded.
‡Air-abraded.
§Pile was used previously in this study as fresh MS or SS. SPT: as standard penetration test, delivering up to 475 Joules/blow with 60–70% energy rating. Failure defined at peak.

Table 7. Pile capacities for Blessington

Pile ID	Time: days	Capacity: kN	Pile	Driving energy	Plug length ratio (PLR)
MS4	2	54·3	MS*	Variable	0·35
MS3	21	55·8	MS*	Variable	0·39
MS2	78	50·3	MS*	Variable	0·34
MS1	121	—	MS*	Variable	0·45
GS4	2	52·8	GS	Variable	0·21
GS3	21	50·3	GS	Variable	0·22
GS2	78	56·8	GS	Variable	0·23
GS1B	121	—	GS	Variable	0·19

*Pre-corroded. Failure defined at peak.

blow-count envelopes. The fresh MS and SS piles developed mean PLRs $\approx 43\%$ irrespective of energy levels, while the shot-blasted SS piles' mean PLR was slightly lower (38%) and the pre-corroded MS piles had a significantly lower mean PLR $\approx 22\%$; see Table 6.

The Blessington piles required ≈ 90 blows with the post-driving system to achieve initial 0·5 m embedments before effectively refusing to advance. However, as shown in Fig. 12(c), only 15–20 further blows were required to complete penetration on the following day with the 4 t hammer (falling 200 mm) imparting far larger energies (up to 5000 Joules/blow) and developing greater final sets (≈ 60 mm, or one diameter/blow) than those (74 to 330 Joules/blow and 5 to 10 mm sets) realised at Larvik and Dunkirk. The average PLRs of the GS piles were lower than for the MS cases (21 and 36%, respectively), possibly reflecting higher interior roughnesses for the GS piles; see Table 7.

Static load–displacement behaviour

The static test results are summarised in Tables 5–7 and representative load–displacement curves are presented in Figs 13(a)–13(c). The Larvik piles developed ductile plateaux after around 6 mm ($\approx 12\%$ of OD), see Fig. 13(a). However, the Blessington and Dunkirk piles' displacements at peak load exceeded the 10% OD limit at which capacities are often defined. The larger piles driven at all three sites required notably smaller normalised displacements to reach tension failure. The resistances of the Blessington and Dunkirk micro-piles' capacities were comparable, and up to 20 times those available in the silty, loose and submerged Larvik sand. The Larvik MS piles showed gains in capacity with time, as well as a tendency for initial stiffness to increase. The Dunkirk MS piles also set-up markedly, but indicated no systematic increase in axial stiffness, mirroring the larger diameter Dunkirk tests; Jardine *et al.* (2006). The Blessington piles showed little change in capacity or stiffness with age but softened post-peak; the Larvik and Dunkirk piles' responses were ductile.

Shaft capacity trends with time

The micro-piles' peak tension capacities, normalised by those of pre-corroded MS piles at the 1 to 2 day age, are presented in Figs 14(a)–14(c). (The fresh MS and all SS Dunkirk piles had smoother surfaces than the other piles, and the pre-corroded MS Dunkirk piles matched better the Larvik, Blessington and typical industrial pile conditions.) Capacities are based on maximum recorded loads corrected for pile and plug weights; no reverse end bearing is considered.

The pre-corroded MS piles driven at Larvik showed, after 315 to 696 days, upper limit capacities $\approx 2\cdot2$ times the 1 day reference value. Their set-up factor fell below the equivalent ratio ($\approx 2\cdot9$) found from the 508 mm OD piles after 200 days; see Fig. 1. In contrast to the MS piles, the SS Larvik piles' capacities remained at the pre-corroded MS pile's day 1 capacity. The apparent test scatter reflects the tendencies of the 'east-end' piles 12 and 6 to plot above the 'west-end' piles 3, 4 and 5 because the mean CPT q_c values tend to increase by $\approx 15\%$ west to east across the test area; the relatively low capacity of pile 2 reflects its lower period of on-site exposure, pre-corrosion and roughening before driving.

The Dunkirk tests investigated capacity variations between the fresh MS, pre-corroded MS, initially smooth SS and air-abraded SS piles. As shown in Fig. 14(b), the fresh MS and the SS piles did not set-up significantly over the first day after driving. However, the capacity of a pre-corroded MS pile tested at 1 day (R1) was 1·5 to 1·8 times higher than that of a relatively smooth fresh MS pile at similar age (S1, S2, S19, S20). Increasing the shaft roughness boosts initial static capacity (and reduces driving PLR) significantly; see Tables 4 and 6. The pre-corroded MS and fresh MS Dunkirk piles all developed long-term capacity growth. Despite scatter, the trend lines show steeper (semi-logarithmic) medium-term gains for the fresh MS piles.
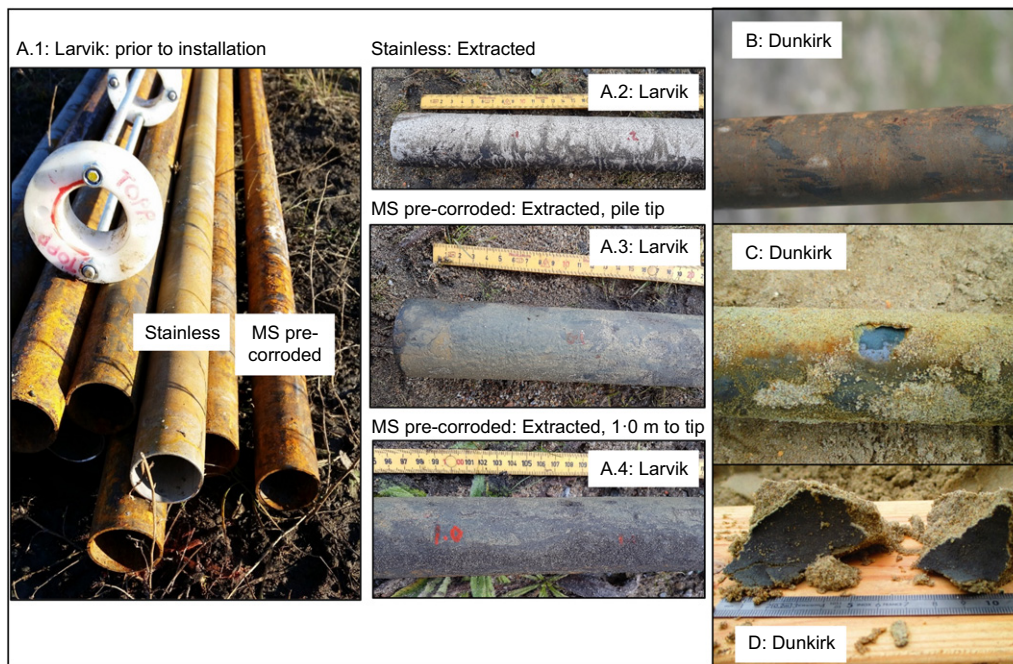
Fig. 8. (Label A.1) Larvik pre-corroded MS and stainless steel piles, before use November 2015; (labels A.2–A.4) Larvik extracted piles, pulled out October 2017; (label B) Dunkirk pre-corroded pile before use; (label C) Dunkirk fresh MS extracted pile, dug out; and (label D) Dunkirk oxidised sand taken from face of a MS pile after extraction
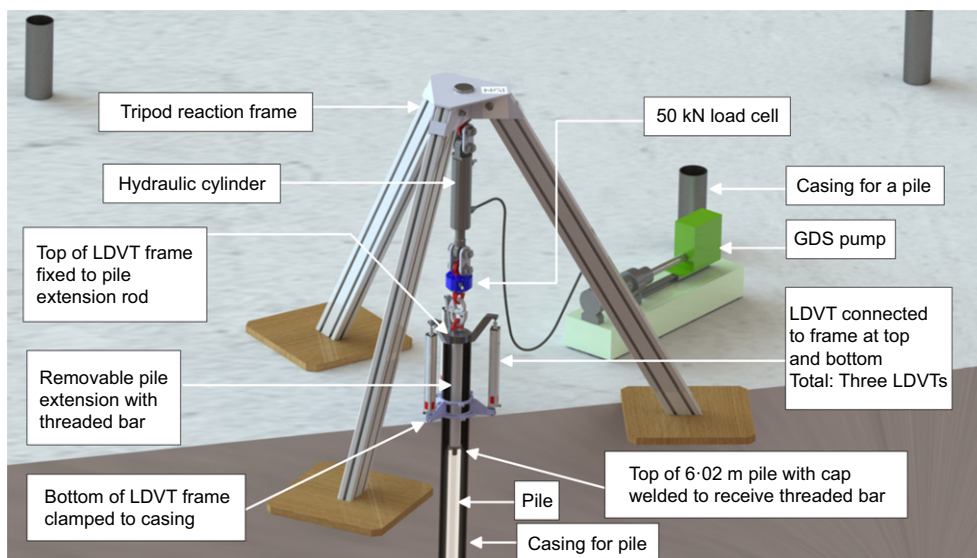

Fig. 9. Larvik tension test set-up

It is interesting that the pre-corroded and fresh MS piles both tend towards maxima around 1·4 to 1·6 times the 1 day reference (pre-corroded) capacity. However, the latter ratios are lower than the $\approx 2 \cdot 2$ ratio seen with the Larvik micro-piles and far below the 2·9 to 3·7 gains seen with larger piles at Larvik and Dunkirk, respectively: see Fig. 1. As at Larvik, the Dunkirk SS piles showed no set-up. The SS piles delivered similar capacities after undergoing air-abrasion, confirming that this treatment had not modified their relatively hard surfaces as significantly as had been intended.

The equivalent trends for Blessington are presented in Fig. 14(c). It is noteworthy that the MS or GS piles driven with the 4 t hammer developed practically the same capacities and, unlike the larger piles illustrated in Fig. 1, no set-up.

Average shaft shear resistances

It is instructive to consider the piles' average failure shaft shear resistance (τ_{avg}) variations with time in Figs 15(a)–15(c). Also plotted in Fig. 15 are the τ_{avg} average shaft shear resistances from the larger piles reported in Fig. 1 and the average sleeve friction resistance (f_s) over the embedment interval from the closest CPTs, which vary from ≈ 20 kPa for Larvik to ≈ 150 kPa at Dunkirk and Blessington. Despite the piles' open ends and the geometrical (h/R^*) or 'friction fatigue' factors identified from
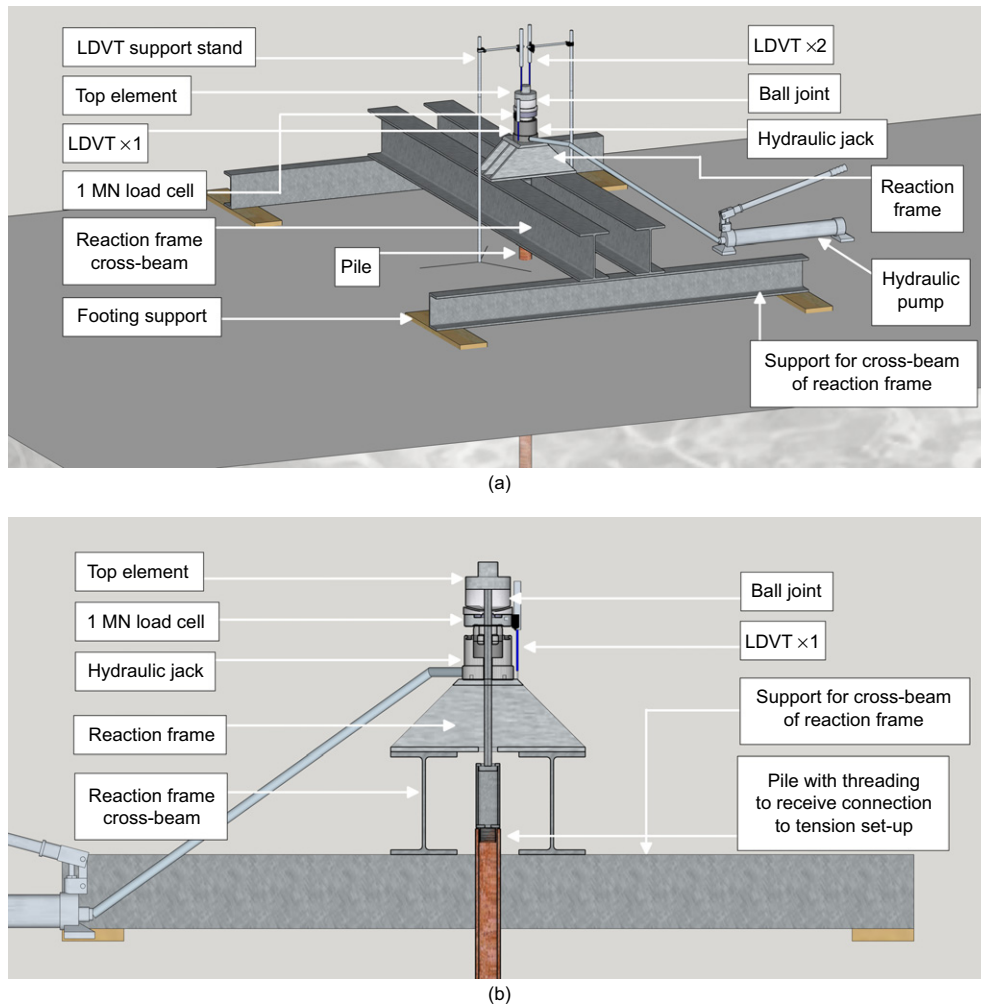
(a)

(b)

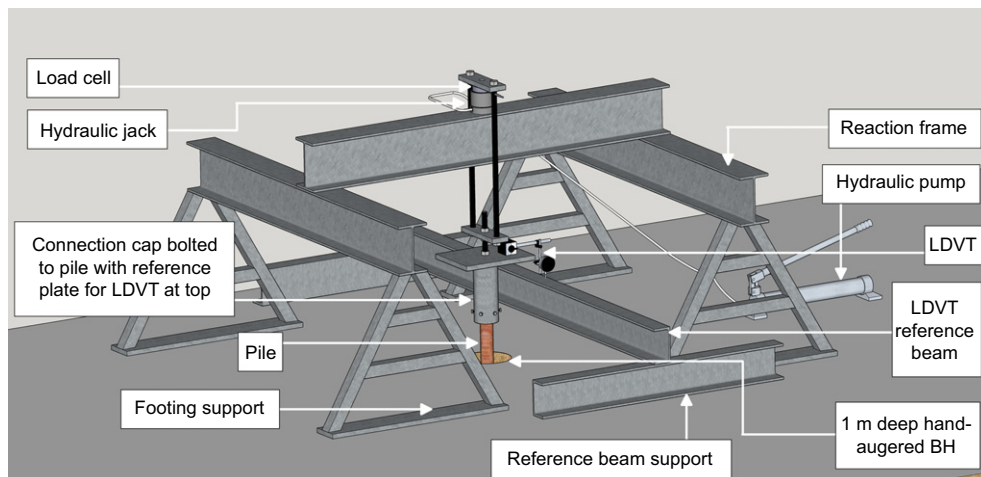**Fig. 10. (a) Dunkirk tension test set-up. (b) Close-up of Dunkirk test set-up**

Fig. 11. Blessington tension test set-up

instrumented field tests in sands, the pre- corroded rough micro-piles' τ_{avg} resistances exceed or match f_s from day 1 at Dunkirk and Blessington, but only climb towards $0.75\,f_s$ after a year at Larvik.

The Larvik MS micro-piles developed markedly lower average resistances at all ages than equivalent 508 mm diameter piles, which may reflect partially the higher CPT q_c values applying over the larger piles' shafts. The opposite

applied at Dunkirk where the MS micro-piles developed higher resistances at all ages, despite their shallow depths.

It is interesting that the Blessington micro-piles achieved, in a less variable q_c profile, short-term shaft capacities that matched the long-term upper limit achieved by the large piles and also the average f_s values developed in the monotonically jacked CPT tests. The shaft ageing outcomes found with these relatively long ($L/D = 29.2$) micro-piles are compatible
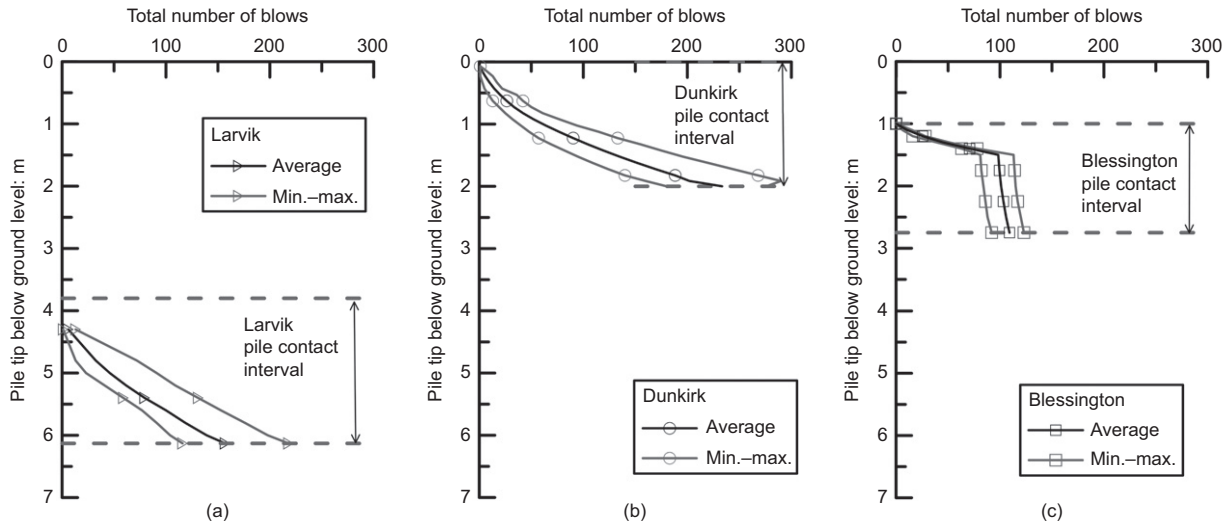
Fig. 12. (a) Total number of blows plotted against depth at Larvik. (b) Total number of blows plotted against depth at Dunkirk (SPT and variable energy driving). (c) Total number of blows plotted against depth at Blessington

with the hypothesis posed in the introduction that upper limits may apply that cap the shaft resistance, and therefore the radial effective stresses that can develop, despite further corrosion, shaft roughening or any otherwise potentially beneficial ongoing ageing process. The only special feature of the piles that may have led to their limiting capacities being reached very early after driving was the much higher driving energy, and therefore large penetration for a given blow, imparted by the 4 t hammer.

Capacity normalisation

Further insights can be gained by normalising the measured capacities with capacity predictions from design procedures that account for site and pile characteristics. While the Larvik piles were submerged, even small suctions could be important to the Dunkirk and Blessington micro-piles and their σ'_{v0} profiles have been assessed by treating the profiles as if saturated and adding the measured suctions to the total vertical stresses.

The API (2011) main text method assumes that local $\tau_f = \beta\,\sigma'_{vo}$ where σ'_{v0} is the free-field effective stress. An upper-bound τ_f applies to API (2011) that depends (with β) on in situ relative density and grain size. API (2011) is not applicable to loose sands, so the previous API (1993) version has been applied to the Larvik pile cases. The NGI-05 method uses q_c as the main soil input parameter to determine local relative density, which together with σ'_{v0} controls shaft resistance. The NGI-05 and API main text methods do not link τ_f to pile diameter, G or shaft roughness.

The alternative ICP-05 method was developed from field experiments with 102 mm dia. instrumented jacked piles, installed to depths of up to 6 m in loose dune sand (Lehane *et al.*, 1993) and dense marine sand (Chow, 1997). Local stress sensor measurements of shear and radial stresses plus pore pressures, combined with experiments on larger instrumented open pipe-piles showed that the shaft failures achieved in tension tests conducted within days of installation could be matched by three equations

$$\tau_f = \sigma'_{rf}\tan(\delta_{cv}) \tag{1}$$

with

$$\sigma'_{rf} \approx (0{\cdot}8\sigma'_{rc} + \Delta\sigma'_{rd}) \tag{2}$$

and

$$\sigma'_{rc} \approx 0{\cdot}029 q_c (\sigma'_{v0}/P_a)^{0{\cdot}13}(h/R*)^{-0{\cdot}38} \tag{3}$$

where τ_f is the local shear stress at failure; δ_{cv} is the ultimate interface shearing angle; h is the depth of the pile tip below the point in question; and $R* = (R_{outer}^2 - R_{inner}^2)^{0{\cdot}5}$. Interface ring-shear tests show that δ_{cv} reduces with sand D_{50} and increases with interface average centre-line roughness R_{cla}; Ho *et al.* (2011). Similar tests on samples from all three sites with appropriate interfaces and stress levels gave the angles indicated in Table 2. The radial effective stress acting on the pile shaft at failure, σ'_{rf} is related to

(a) σ'_{rc} the equalised shaft radial effective stress, which depends weakly on σ'_{v0}, increases directly with q_c and reduces with normalised pile tip depth, $h/R*$

(b) the change in shaft stress $\Delta\sigma'_{rd}$, due to constrained outward radial movements related to dilation at the interface. The reviews of Lehane (1992) and Chow (1997) of available field and laboratory model test data for sands indicated that equation (4) provides suitable estimates for $\Delta\sigma'_{rd}$ when the dilative radial displacement is taken as equal to the average peak-to-trough roughness, $2R_{cla}$

$$\Delta\sigma'_{rd} = 4GR_{cla}/D \tag{4}$$

While $\Delta\sigma'_{rd}$ values are hard to evaluate precisely, equation (4) indicates that dilation offers relatively modest contributions (often less than 5%) to the medium-term capacities of large-diameter industrial piles. However, Axelsson (2000) and Gavin *et al.* (2013, 2015) argue that the 'dilative' term contributes far more significantly to aged industrial piles. It also has the potential to dominate the frictional resistance of micro-piles. While Jardine *et al.* (2005) suggest a default $R_{cla} \approx 10\,\mu m$ estimate for industrial steel piles, the case-specific values assessed for the present study are summarised in Table 4. Radial movements greater than double the initial R_{cla} could be generated on loading after any corrosion in situ and/or bonding with sand particles. It is also possible that movements lower than $2R_{cla}$ could apply in any very loose, silty/clayey sands that contract when sheared.

The operational (in situ) sand shear stiffness G is also difficult to select, especially for micro-piles driven above the water table. The expressions of Jardine *et al.* (2005) for G_{max} as a function of q_c were applied at Larvik, while the seismic
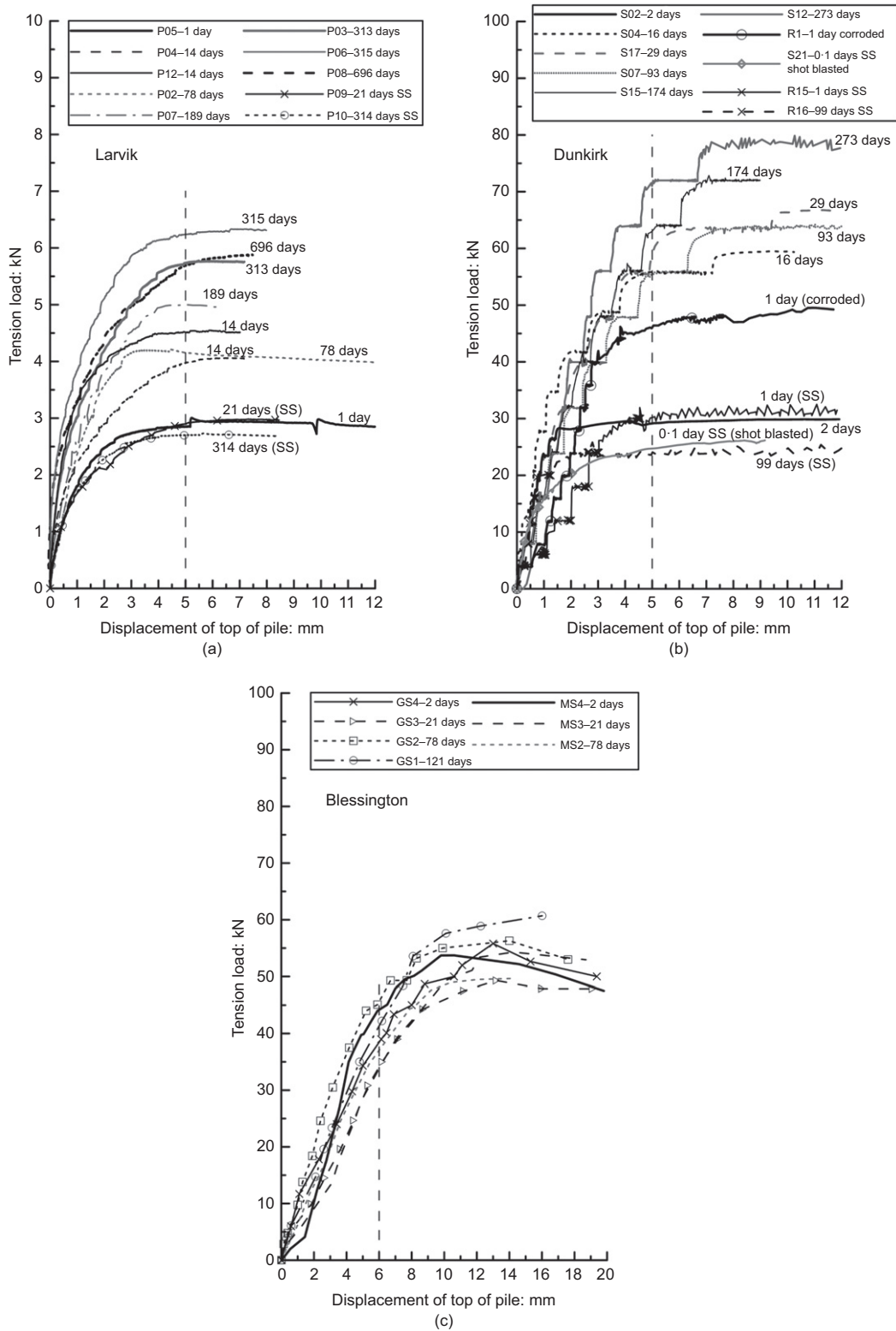
Fig. 13. (a) Tension load plotted against displacement for selected tests with 10% pile diameter marker at Larvik. (b) Tension load plotted against displacement for selected tests with 10% pile diameter marker at Dunkirk. (c) Tension load plotted against displacement for selected tests with 10% pile diameter marker at Blessington

CPT and MASW measurements made at Dunkirk and Blessington provided direct information on the undisturbed in situ G_{max} profile. The operational values would be raised by the effective stress changes generated by pile installation (particularly at Dunkirk and Blessington), and would be affected by anisotropy or reduced if the response to shaft loading to failure is non-linear; Jardine *et al.* (2013). The

radial cavity strain ($\delta_{R/R}$) required at the shaft for the sand to unlock from the shaft and allow failure to occur is $4R_{cla}/D$, which amounts to $\approx 0.08\%$ for the rougher micro-piles and exceeds the linear range of most sands. Assuming similar roughness values, the corresponding strains would be up to 10 times lower for the larger piles tested earlier at the same sites.
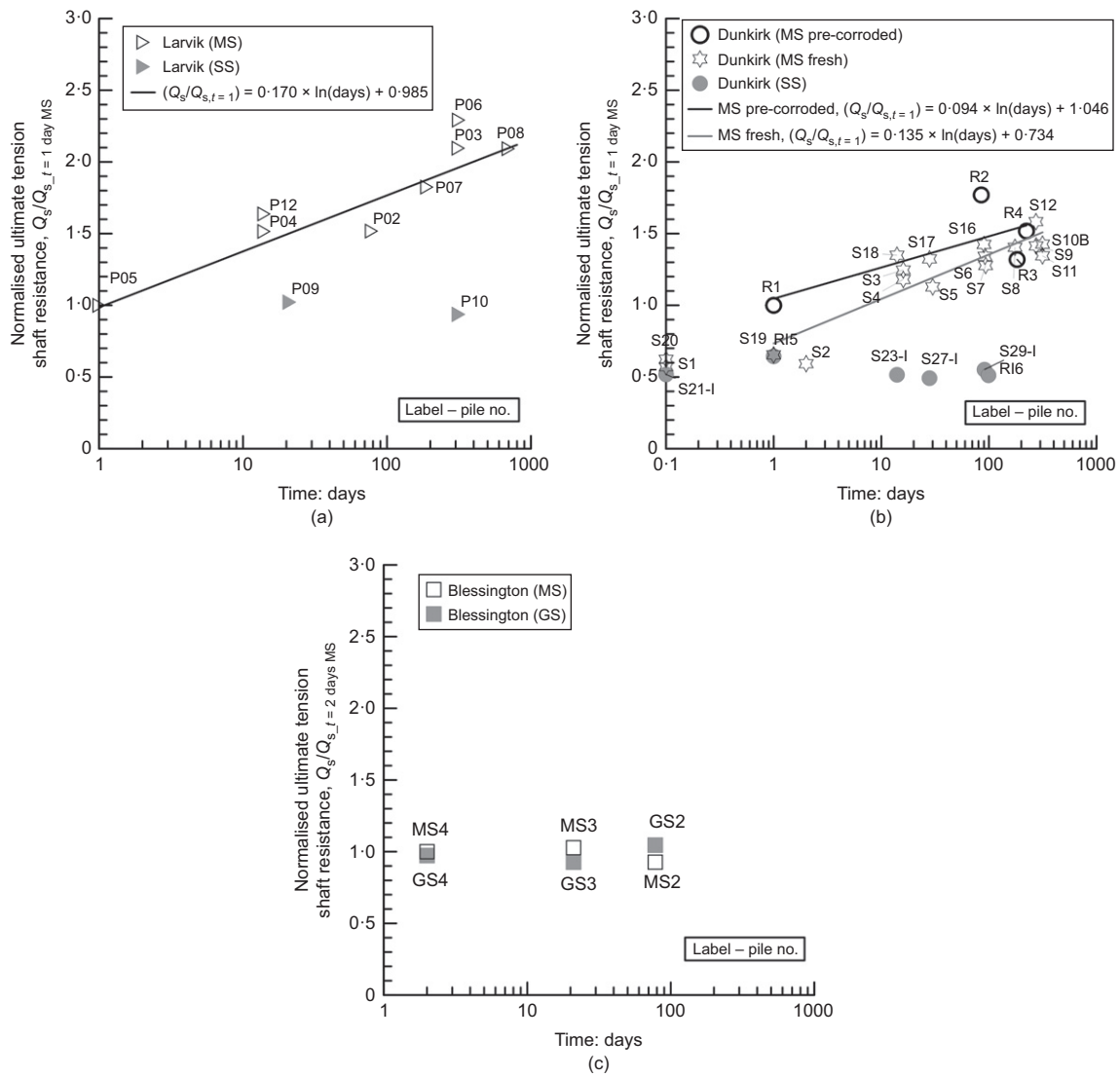
Fig. 14. (a) Normalised ultimate tension shaft resistance based on peak pile capacity for pre-corroded pile $Q_s/Q_{s\_t=1\ day\ MS}$ at Larvik. (b) Normalised ultimate tension shaft resistance based on peak pile capacity for pre-corroded pile $Q_s/Q_{s\_t=1\ day\ MS}$ at Dunkirk. (c) Normalised ultimate tension shaft resistance based on peak pile capacity for pre-corroded pile $Q_s/Q_{s\_t=2\ day\ MS}$ at Blessington

The ICP-05 approach allows estimates to be made for how driven pile installation and interface dilation affect shaft radial effective stresses. However, the micro-piles are smaller, and involve lower initial effective stresses, than all previous field evaluations of the method and the predictions are inevitably subject to uncertainty.

Tables 2 and 8 list the input parameters considered appropriate for the micro-piles at various test stages and the tension capacities (Q_{sc}) calculated for all three sites. Table 8 also indicates how much of each ICP-05 capacity estimate derives from $\Delta\sigma'_{rd}$ through equation (4), expressed as a ratio of $\Delta\sigma'_{rd}\tan(\delta_{cv})$ to the total calculated capacity. Table 9 lists the corresponding average capacities as measured (Q_{sm}) after 1, 85–100 and 175–315 days and gives Q_{sm}/Q_{sc} ratios for the various cases. Figs 16(a)–16(c) plot the Q_{sm}/Q_{sc} ratio for each pile tested at the three sites, including the IAC curve from Fig. 1.

The loose Larvik sand site is considered first, where 5 to 20% silt contents led to positive excess piezocone pore pressures at some depths (see Fig. 4). The early age micro-pile capacities are over-predicted by API (1993) and marginally under-predicted by NGI-05. As noted earlier, the Larvik MS micro-piles showed marked set-up over the months after driving, but to a lesser degree than the large piles shown in

Fig. 1. ICP-05 predictions made with the default G–q_c function greatly over-predict the micro-piles' initial resistances, giving $Q_{sm}/Q_{sc} = 0.23$, in contrast with the method's more representative prediction for the 508 mm Larvik piles short- to medium-term capacities; see Figs 16(a) and 1. The $\Delta\sigma'_{rd}$ component (see equation (4)) provides 85% of the micro-pile capacity predicted with ICP-05 (see Table 8) and less than 10% for the 508 mm dia. cases, so the over-prediction for Larvik must relate primarily to the dilatant term. Although earlier field tests demonstrated highly significant constrained dilation in clean loose sands (Lehane *et al.*, 1993), a 91% reduction is required in the $\Delta\sigma'_{rd}$ component given by equation (4) to match the micro-pile capacity seen in the 1 to 2 day tests performed in the loose, silty and contractive Larvik sands.

Moving to the Dunkirk dense sand site, it is recalled first that applying the criteria proposed by Emerson *et al.* (2008) indicates that the Dunkirk CPT traces may have been subject to near-surface effects down to depths of 1·5 m; the latter may also have affected the pile test outcomes. However, the micro-piles' capacities were 9·9 times greater at day 1 than expected by API (2011) and 1·6 to 1·8 times greater than estimated by ICP-05 or NGI-05. The SS micro-piles also showed higher capacities than expected, although their
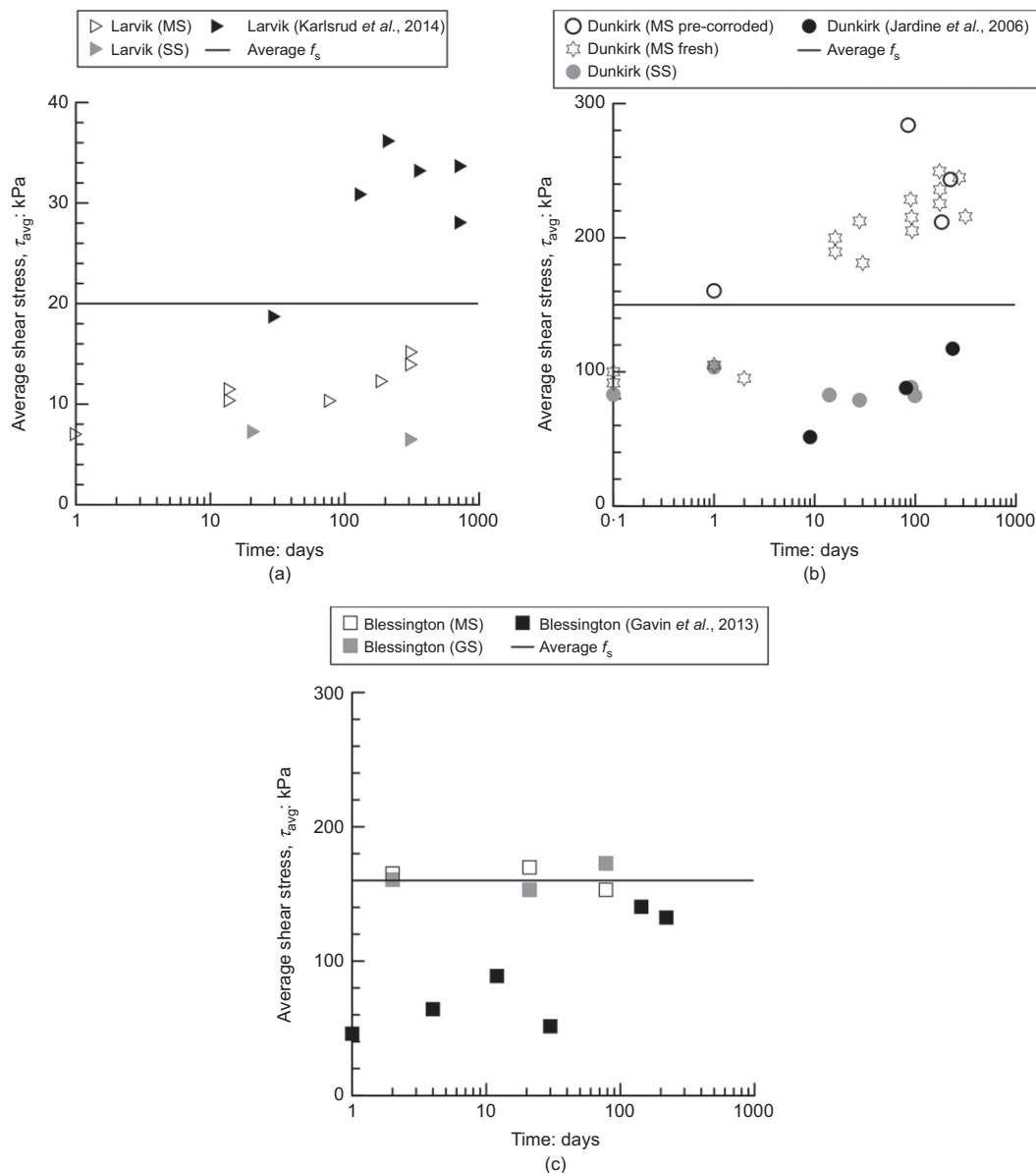
Fig. 15. (a) Average shear stress with time, small and larger diameter piles at Larvik. (b) Average shear stress with time, small and larger diameter piles at Dunkirk. (c) Average shear stress with time, small and larger diameter piles at Blessington

Table 8. Parameters and pile tension capacity predictions based on average of all CPTs

Site	δ_{cv}: deg	β (API)	D_{50}: mm	R_{cla}: μm	ICP‡: kN	API: kN	NGI: kN
Larvik	27·8	0·21	0·25	8·5	11·2 (85%)	4·4§	2·2
Dunkirk*	27·5	0·56	0·26	10·0	30·1 (47%)	5·1	27·9
Dunkirk†	27·5	0·56	0·26	2·0	18·9 (15%)	5·1	27·9
Blessington	29·4	0·46	0·15	10·0	27·0 (52%)	7·2	27·5

*Pre-corroded MS piles and fresh MS > 10 days.
†Fresh MS < 10 day, air-abraded SS and SS.
‡ICP: values in parentheses correspond to ratio of the capacity component term $\Delta\sigma'_{rd} \times \tan(\delta_{cv})$ to the total calculated capacity.
§API: The Larvik analysis applies API (1993) as API (2011) does not apply to loose sands.

Q_{sm}/Q_{sc} ratios remained fixed at $\approx 1·5$ over time. ICP-05 calculations run for closed-ended conditions increased shaft capacity by just 6%, indicating that the micro-piles' relatively low PLRs were not the main cause of the discrepancies. Interface constrained dilation and the diameter-dependent $\Delta\sigma'_{rd}$ term (equation (4)) is expected to contribute around half of the shaft capacity and higher than undisturbed in situ

operational shear stiffness or shaft roughness again appear to be more likely contributors to the ICP-05's initial under-prediction. The Dunkirk MS micro-piles' capacities grew with age although, as at Larvik, their final relative set-up factors were lower than those earlier with larger (457 mm OD) piles shown in Fig. 1. The relatively large relative displacements (see Fig. 13) required to reach micro-pile shaft

Table 9. Tension capacity analysis for MS piles: measured-to-calculated ratios for three methods

	Days	Capacity measured*: kN			ICP-05 Q_{sm}/Q_{sc}			API Q_{sm}/Q_{sc}			NGI-05 Q_{sm}/Q_{sc}		
		Larvik	Dunk.	Bless.	Larvik	Dunk.	Bless.	Larvik	Dunk.	Bless.	Larvik	Dunk.	Bless.
Pre-corroded	1–2	2·6	50	55	0·23	1·67	2·02	0·59	9·80	7·64	1·18	1·79	2·00
Fresh	1–2	—	33	—	—	1·75	—	—	6·47	—	—	1·18	—
Pre-corroded	85–100	4·2	89	56	0·38	2·96	2·07	0·95	17·5	7·78	1·91	3·20	2·04
Fresh	85–100	—	68	—	—	2·26	—	—	13·3	—	—	2·44	—
Pre-corroded	175–315	5·4	71	—	0·48	2·36	—	1·23	13·9	—	2·45	2·54	—
Fresh	175–315	—	74	—	—	2·46	—	—	14·5	—	—	2·65	—

* Average values are presented for the range of days considered for each set of pile types and site.

failure are consistent with constrained dilation (equation (4)) playing a progressively more significant role over time at Dunkirk. The ultimate capacities of the MS piles lead to ICP-05 Q_{sm}/Q_{sc} ratios that scatter around 2·1 to 2·6, similar to the larger piles' trend, as shown in Fig. 16(b). The roughness of the fresh MS piles is assumed to change with time and R_{cla} is assumed $= 10$ μm after 14 days in-place of the initial 2 μm.

The Blessington micro-piles' capacities amounted to 7·7 times the conventional API (2011) estimate and double the NGI-05 estimate. They are $\approx 2·1$ those expected from ICP-05 and remain unchanged with age, falling 15% below the long-term ICP Q_{sm}/Q_{sc} ratio of $\approx 2·5$ given by the larger piles in Fig. 16(c). If the long-term capacity is subject to an upper limit, as postulated by Jardine *et al*. (2006), Lim & Lehane (2014), Rimoy *et al*. (2015) and Gavin *et al*. (2015), this limit appears to have been reached shortly after driving and to have remained unaffected by any subsequent physicochemical or other ageing process. The reasons for this outcome remain open to speculation. However, as noted earlier, the energy used to drive these piles by the 4 t hammer advanced the Blessington micro-piles rapidly by a full diameter per blow, in a manner similar to pile jacking. Gavin & O'Kelly (2007) showed that pile installation resistance at this site is strongly affected by the installation method, with piles installed with long jacking strokes developing shaft capacities close to the f_s values measured in the CPT test. The large axial displacements (up to 30% of OD) required to reach tension failure are compatible with the sand's high δ_{cv} values (see Table 2) and the suggestion that the interface dilation components (equation (4)) of shaft resistance were greater than expected from the ICP-05 calculations.

AGEING MECHANISMS

The micro-pile experiments provide insights on how a range of potential factors affect shaft capacity growth with age.

Cycles in environmental conditions

Considering first the effects of external environmental factors, the absence of set-up for SS or GS piles at any of the three sites demonstrates that diurnal, seasonal or soil microstructural changes had no independent effect on pile ageing processes.

Physicochemical factors

The physicochemical hypothesis was tested by varying the pile steel materials. Paired MS and SS (or GS) piles driven with similar initial roughnesses developed compatible initial capacities that varied between sites, reflecting soil conditions, pile dimensions and roughness' values. However, set-up only took place with the MS micro-piles at Larvik and Dunkirk, proving that physicochemical processes were dominant with these small corrodible piles. Although reaction rates may depend on pile surface specific area and condition, ground temperature, chemistry and oxygen supply levels, their resulting impact on capacity appeared to develop at similar overall rates under conditions ranging from the acidic, loose, silty and submerged Larvik sand, to the vadose zone of the dense, clean, alkaline Dunkirk sand.

Grain scale phenomena close to the pile shafts

Noting that little or no crushing is likely to have developed below the Larvik piles' tips in the low q_c sands present, grain
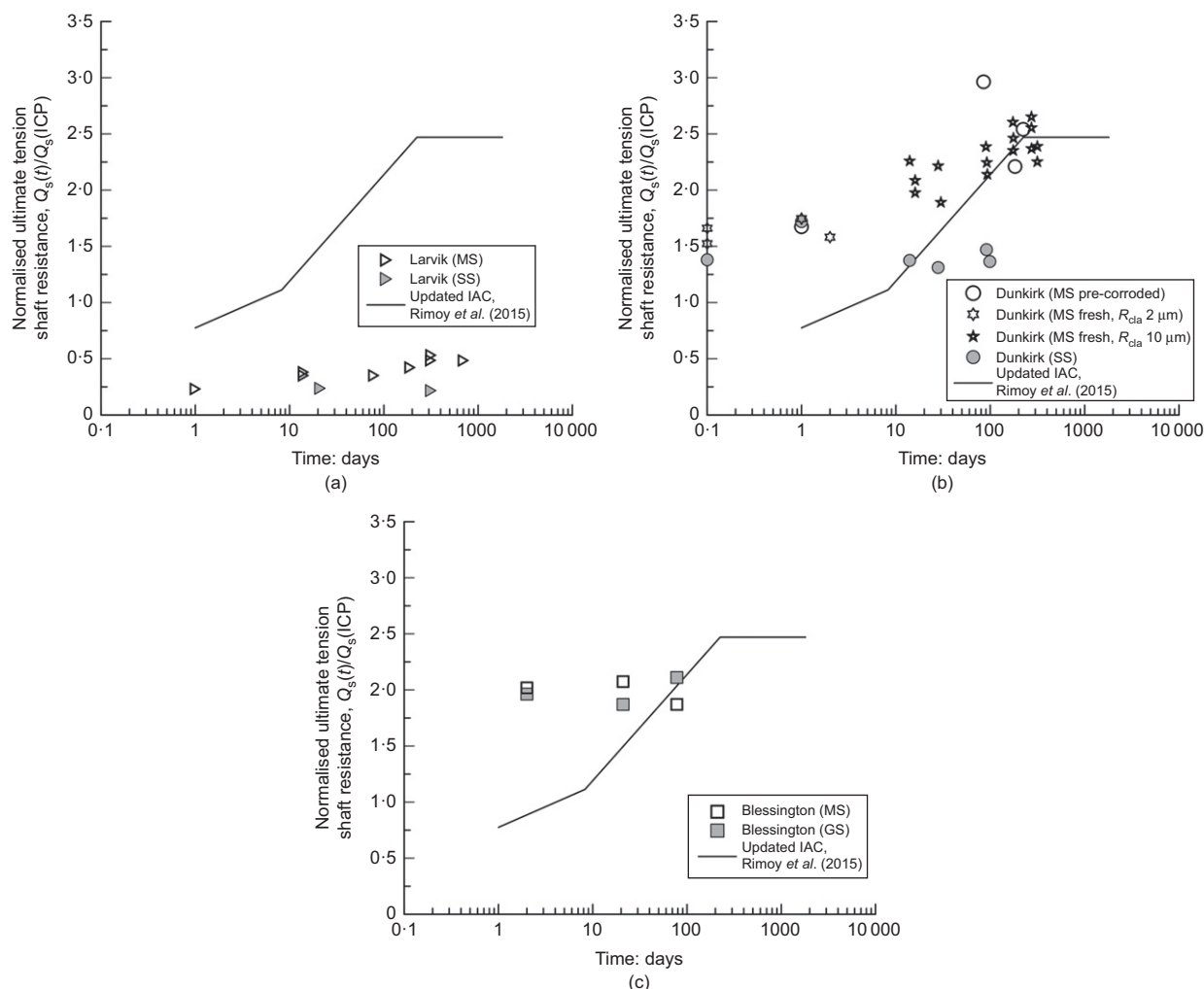
Fig. 16. (a) Ageing trends of micro-piles and 508 mm OD piles driven at Larvik, showing latters' updated IAC. (b) Ageing trends of micro-piles and 457 mm OD piles driven at Dunkirk, showing latters' updated IAC. (c) Ageing trends of micro-piles and 340 mm OD piles driven at Blessington, showing latters' updated IAC

crushing does not appear to have been a necessary condition for the physicochemical ageing processes to apply to the micro-piles or earlier larger (508 mm) diameter piles. However, the early-age tests on pre-corroded micro-piles proved that surface roughening provides a significant part of the capacity growth, principally through enhanced dilation. The pre-corroded MS piles consequently showed less capacity growth over time at Dunkirk than initially smooth MS piles, as both tended to similar upper limits.

Corrosion reactions could also cause additional growth in static radial stresses due to expansion of the pile volume as corrosion products crystallise at the shaft. Modification of the shaft, as shown in Fig. 8, and iron compound cementing also provide a marginally higher effective diameter, probably augmented dilation and δ_{cv} angles that may approach the peak or critical state soil–soil ϕ'_{cs} values. A shift to ϕ'_{cs} would offer a $\tan\phi'_{cs}/\tan\delta_{cv}$ capacity contribution which might provide an additional ≈ 25–35% in silica sands for piles of any diameter.

Enhanced dilation under loading

Instrumented field tests show that constrained dilation under loading contributes to shaft capacity in sands. Axelsson (2000) and Gavin et al. (2013) observed that it contributed to capacity growth over time with industrial concrete and steel driven piles. The shapes of the Dunkirk

MS micro-piles' load–displacement curves also indicate that interface dilation became more important with time. However, no set-up or displacement to failure growth applied to the SS and GS micro-piles, so physicochemical processes involving mild steel (or concrete) are required to generate any additional radial movements that might contribute to raising the shaft stresses in combination with any shift from the interface shear angle rising from δ_{cv} towards ϕ'_{cs}.

Evidence obtained by comparing piles with different diameters

Set-up appears to be diameter dependent: the micro-piles all developed lower relative gains than the larger piles tested earlier at the same site. The corrosion reactions observed around the pile shafts can be expected to advance at rates that are independent of the piles' diameters. Micro-piles and larger industrial piles can therefore be expected to show similar absolute gains in effective diameter and absolute additional radial movements due to dilation when loaded to failure. The relative impact of these changes on shaft capacity should all diminish with increasing pile diameter, as indicated by equation (4), rather than follow the opposite trend seen in the field experiments. Recalling from Fig. 2(a) that industrial concrete piles also set-up and that capacity gains have been observed over relatively short times with offshore piles driven in sands to penetrations where the

oxygen supply is severely limited (Jardine *et al.*, 2015), it appears that steel corrosion cannot be the only process at work. Other factors must be operating whose impact is greater with larger diameter piles.

Radial stress redistribution

It remains highly challenging to undertake analyses of installation in sand that explore the generated in situ stress fields quantitatively. However, Yang *et al.* (2014) and Zhang *et al.* (2014) show that an arching stress field can be expected to develop in sands around even monotonically penetrating piles. The SS and GS micro-pile experiments confirm the postulate of Rimoy *et al.* (2015) that radial stress redistribution does not contribute significantly to micro-pile ageing. However, the redistribution mechanism may be more effective around larger open-ended driven piles which involve higher: (*a*) initial stresses, (*b*) ratios of diameter *D* to crushed-sand bandwidth, (*c*) *D* to wall thickness, *t*, ratios, (*d*) final PLRs and (*e*) total blow-counts. The grain crushing, dynamic load cycling and shear band formation that take place when industrial piles with high *D/t* ratios are driven may all accentuate arching around the shaft and provide greater scope for stress redistribution and capacity growth over time and contribute to the set-up observed shortly after driving (in significant water depths) for large offshore piles in dense sands.

Pile driving technique

It has been argued that the lack of set-up, even by physicochemical processes, of the MS Blessington piles was related to employing an oversized hammer over their main drive lengths, which led to installation conditions similar to pile-jacking, with penetrations of one full diameter per blow, and contrasted strongly with the conventional driving of the 340 mm OD piles, which manifested the strong set-up seen in Fig. 1. Other tests at Blessington by Chatta (2006) on 73 mm OD closed-ended piles installed with both 1 m and 50 mm jack strokes and tests with 75, 100 and 114 mm OD open-ended piles driven (with high blow-counts) by an SPT hammer (Gavin *et al.*, 2003) confirm that the installation procedure affects both PLRs and short-term capacity. Hard driving reduces the radial effective stresses around the shaft and leaves greater scope for capacity growth than the micro-piles' high-energy installation, which delivered unusually high short-term capacities that fell close to the upper limits suggested by Figs 1 and 16.

Possible upper limit to aged shaft capacities

The tests at all three sites support the hypothesis that an upper limit applies to aged shaft capacity which amounts to 2·1 to 2·5 times the ICP-05 predictions, irrespective of any ongoing ageing process.

CONCLUSIONS

Fifty-one co-ordinated static first-time tension tests have been reported, along with site investigations, on open-ended steel micro-piles failed at ages between 0·1 and 696 days, at sand sites covering loose to dense conditions and varying silt contents. Fresh, smooth and pre-corroded, rough, mild steel, stainless and galvanised steel piles were considered. Integration with earlier larger diameter pile tests and an independent database study allowed investigation of how pile diameter, steel corrodibility, surface roughness and ground conditions affect ageing behaviour. The influence of driving procedure was also considered. Reflecting the key questions posed in the introduction, three groups of conclusions are drawn.

Group 1: pile material, roughness and physicochemical processes were found to be highly influential to ageing.

(*a*) Physicochemical processes dominated the marked set-up shown by mild steel micro-piles in submerged silty, loose (Larvik) sand and clean, dense unsaturated (Dunkirk) sand.

(*b*) No set-up was seen with non-corrodible stainless or galvanised steel piles, so no independent ageing process, such as radial stress re-distribution, growth of shear stiffness, dilation due to creep or enhanced grain interlocking affected the micro-piles significantly in the absence of physicochemical effects.

(*c*) The physicochemical processes identified as potentially affecting ageing include: (i) pile surface roughness increasing through redox reactions; (ii) bonding between sand and corroding shaft; (iii) marginally higher effective diameters; (iv) interface shear angles rising towards the ϕ'_{cs} limit; and (v) growth in static radial stress σ'_{rc} due to radial expansion of the corroding steel.

(*d*) However, the database studies outlined in Fig. 2 and the Appendix show that concrete and steel piles with diameters between 0·2 and 1·3 m gain capacity at similar rates over time. Steel corrosion reactions cannot be the only mechanism that leads to set-up with larger piles driven in sands.

(*e*) Pile roughness and constrained dilation had a critical effect on the micro-piles' capacities.

Group 2: four further key points emerged concerning the specific piles and sites investigated.

(*a*) The mild steel micro-piles developed lower set-up factors than the larger industrial piles tested previously at the Larvik, Dunkirk and Blessington test sites.

(*b*) The lack of set-up shown by stainless steel piles proved that seasonal variations in temperature and/or possibly pore pressures had no independent influence on pile ageing, which also appeared largely independent of the sites' initial geochemical conditions.

(*c*) The micro-pile shaft capacity measurements indicate that the ICP-05 dilation term expressed in equations (2) and (4) gives only an approximate indication of the observed field behaviour. While the impact of dilation is minor for large piles at early ages after driving, the discrepancies are important with micro-piles. The ICP-05 dilation term should be set to zero when assessing short- to medium-term shaft capacities in loose, silty sands that manifest positive piezocone pore pressures. Equally, applying equation (4) as recommended in ICP-05 appears to underestimate significantly the contribution that constrained dilation makes to micro-pile shaft capacity in dense sands.

(*d*) Short-term capacity and set-up depend on the installation process. A range of tests conducted earlier at Blessington confirmed that heavy driving reduces the radial effective stresses available after installation and creates scope for capacity gains over time. However, employing a greatly over-sized hammer for the micro-piles led to capacities that did not change with time and were close at an early age to the upper limit developed after long ageing by conventionally driven piles.

Group 3: considering the third key question as to whether any upper limit applies to shaft capacity, irrespective of any

continuing active ageing processes, the following points can be made.

(a) Upper limits to shaft capacity were found at all three sites, by piles of two scales, that appeared to fall around 2·1 to 2·5 times the capacities estimated by the medium-term ICP-05 procedures when based on best estimates of pile and soil conditions.

(b) While most piles are installed with initial capacities well below this upper limit, a range of ageing processes apply in the field that allow growth over time towards the site-specific maxima, which appear to be controlled by limits to the radial pressures that can be developed around the pile shafts.

(c) Exceptions to the above general trend include: (i) chemically inert stainless steel micro-piles driven in dense Dunkirk sands, which showed no set-up above their initial capacities that fell around 50% above the ICP estimates; (ii) the micro-piles driven in loose, silty and contractant Larvik sand, whose degrees of interface dilation and therefore shaft capacities fell far below those expected.

APPENDIX: PILE AGEING IN SILICA SANDS

See Table 10.

Table 10. Case studies identified by Rimoy et al. (2015)

Reference	Site location	Ground description	Pile description				Load test description
			Material (number of piles)	Average length: m	Section/diameter[†]: m	L/D	Type, direction D/S[†]:, C/T[†]:
Tavenas & Audy (1972) [‡]	St Charles River, Quebec city, Canada	Medium uniform sand	Concrete (28)	11	Hexagonal 0·305	36	S, C
Skov & Denver (1988)	Hamburg, Germany	Sand and silt	Concrete (6)	21	Square 0·395	53	D/S, C
	Südkai, Hamburg Harbour, Germany	Coarse medium to medium fine sand and fine gravel	Steel (1)	33·7	Pipe 0·762	44	D/S, C
Seidel et al. (1988)	Australia	Loose to dense sand	Concrete (1)	11	Square 0·508	21	D/S, C
Zai (1988)	China	Fine sand	Steel (5)	41·4	Pipe 0·609	68	D, C
DiMaggio (1991)	Mobile County, Alabama, USA	Saturated silty sand	Concrete (5)	21·5	Square 0·688	31	D/S, C
Svinkin et al. (1994)	Various sites, USA	Silty clayey fine sand	Concrete (1)	38	Square with void 0·573	66	D/S, C
			Concrete (1)	27·4	Square 0·402	68	
			Steel (1)	25·3	Closed-ended pipe 0·324	78	
York et al. (1994)	JFK international terminal, Jamaica, New York, USA	Organic silty clays and peats underlain by fine to medium glacial sand	Steel (13)	19·9	Open-ended 0·355 tapered to 0·2 over 7·6 m	99·5	D/S, C
			Timber (1)	15·8	N/M	N/A	
			Steel (1)	20·7	Pipe	N/A	
Chow et al. (1998)	Port Autonome de Dunkerque, Dunkerque, France	Medium to dense marine silica sand q_c average 21 MPa	Steel (2)	16·5	Open-ended pipe 0·324	51	D/S, C/T
Axelsson (2000)	Fittja Strait, Vårby, Stockholm, Sweden	Loose to medium dense glacial sand. q_c 2–8 MPa, <50% silica	Concrete (4)	17·4	Square 0·265	65·8	D/S, C

Continued

Table 10. *Continued*

Reference	Site location	Ground description	Pile description				Load test description
			Material (number of piles)	Average length: m	Section/diameter[†]: m	L/D	Type, direction D/S[†]:, C/T[†]:
Fellenius & Altaee (2002)	JFK international terminal, Jamaica, New York, USA	Fine to coarse medium dense to dense glacial sand	Steel (1)	18	Open monotube 0·45	40	D, C
			Steel (1)	18	Open taper tube 0·45–0·2 over 7·6 m	90	D, C
Jardine *et al.* (2006)	Port Autonome de Dunkerque, Dunkerque, France	Medium to dense marine silica sand q_c 20 MPa	Steel (3)	19·02	Open-ended pipe 0·457	41·6	S, T
Rimoy (2013)	Red Sea port development	Dense coral granitic gravels & sands with cementation	Steel (13)	31·8	Open-ended pipe 1·219	26·1	D/S, C
Gavin *et al.* (2013)	Blessington, Ireland	Dense fine glacial sand; q_c 10–20 MPa	Steel (4)	7	Open-ended pipe 0·34	20·6	S, T
Karlsrud *et al.* (2014)	Larvik, Norway	Loose to medium dense clayey silty fine sand	Steel (7)	21·5	Open-ended pipe 0·508	42·3	S, T
	Ryggkollen, Norway	Medium dense medium fine to coarse sand with cobbles	Steel (6)	20	Open-ended pipe 0·406	49·3	S, T

*C, compression; T, tension; D, dynamic testing with PDA and analysed by CAPWAP (Rausche *et al.*, 1985); S, static testing; N/M, not mentioned.

†Further comment on case studies: for piles with non-circular cross-sections the diameter of an equivalent circular cross-section base area is used.

‡Further comment on case studies: Tavenas & Audy's (1972) aged piles capacities were obtained from Fig. 15 of the reference.

NOTATION

D — pile outer diameter
D_r — relative density
D_{50} — size of particle at 50% point on particle distribution curve
D_{90} — size of particle at 90% point on particle distribution curve
f_s — sleeve friction resistance in cone penetration test (CPT) and CPTu
G — operational shear modulus
G_{max} — small-strain shear modulus
h — depth of the pile tip below the point in question along the pile
Q_c — compression capacity
Q_s — tension shaft capacity
Q_{sc} — calculated tension shaft capacity
Q_{sm} — measured tension shaft capacity
q_c — measured cone resistance in CPT and CPTu
R^* — equivalent pile radius for open-ended piles
R_{cla} — centre-line average roughness
t — pile wall thickness
u_2 — pore pressure measured behind the cone in CPTu
z_{crit} — critical depth for shallow CPT
$\Delta\sigma'_{rd}$ — change in radial shaft stress during loading
δ_{cv} — constant volume interface shearing angle
$\delta_{R/R}$ — radial cavity strain
σ'_{rc} — equalised shaft radial effective stress on the pile shaft
σ'_{rf} — radial effective stress on the pile shaft at failure
σ'_{v0} — in situ effective stress
τ_{avg} — piles' average shaft shear resistance at failure
τ_f — local shear stress at failure
ϕ'_{cv} — constant volume angle of shearing resistance
ϕ'_p — peak angle of shearing resistance

REFERENCES

Aghakouchak, A., Sim, W. W. & Jardine, R. J. (2015). Stress-path laboratory tests to characterise the cyclic behaviour of piles driven in sands. *Soils Found.* **55**, No. 5, 917–928.

API (American Petroleum Institute) (1993). *Recommended practice for planning, designing and constructing fixed offshore platforms – working stress design, API RP 2A-WSD*, 20th edn. Washington, DC, USA: API.

API (2011). *Geotechnical and foundation design considerations. Recommended practice 2GEO, Report*. Washington, DC, USA: API.

Åstedt, B., Weiner, L. & Holm, G. (1992). Increase in bearing capacity with time for friction piles in silt and sand. *Proceedings of Nordic geotechnical meeting*, Aalborg, Denmark, pp. 411–416.

Attwooll, W. J., Holloway, D. M., Rollins, K. M., Esrig, M. I., Sakhai, S. & Hemenway, D. (1999). Measured pile set-up during load testing and production piling: I-15 corridor reconstruction project in Salt Lake City, Utah. *Transpn Res. Rec., J. Transpn Res. Board* **1663**, 1–7.

Axelsson, G. (2000). *Long-term set-up of driven piles in sand*. PhD thesis, Royal Institute of Technology, Stockholm, Sweden.

Bea, R. G., Jin, Z., Valle, C. & Ramos, R. (1999). Evaluation of reliability of platform pile foundations. *J. Geotech. Geoenviron. Engng* **125**, No. 8, 696–704.

Boulon, M. & Foray, P. (1986). Physical and numerical simulation of lateral shaft friction along offshore piles in sand. In *Proceedings of the 3rd international conference on numerical methods in offshore piling, Nantes, France*, pp. 127–148. Paris, France: Editions Technip.

BSI (2016). BS EN 10305-3:2016: Steel tubes for precision applications. Technical delivery conditions. Welded cold sized tubes. London, UK: BSI.

Bullock, P. J., Schmertmann, J. H., McVay, M. C. & Townsend, F. C. (2005). Side shear setup. I: test piles driven in Florida. *J. Geotech. Geoenviron. Engng* **131**, No. 3, 292–300.

Byrne, B. W., McAdam, R., Burd, H. J., Houlsby, G. T., Martin, C. M., Zdravković, L., Taborda, D. M. G., Potts, D. M., Jardine, R. J., Sideri, M., Schroeder, F. C., Gavin, K., Doherty, P., Igoe, D., Muir Wood, A., Kallehave, D. & Skov Gretlund, J. (2015). New design methods for large diameter piles under lateral loading for offshore wind

applications. In *Frontiers in offshore geotechnics III* (ed. V. Meyer), vol. 1, pp. 705–710. Leiden, the Netherlands: CRC Press/Balkema (Taylor and Francis Group).

Chatta, I. (2006). *Investigation of installation effects and cyclic loading on piles in sand*. MS thesis, University College Dublin, Dublin, Ireland.

Chow, F. C. (1997). *Investigations into displacement pile behaviour for offshore foundations*. London, UK: University of London (Imperial College).

Chow, F. C., Jardine, R. J., Brucy, F. & Nauroy, J. F. (1998). Effects of time on capacity of pipe piles in dense marine sands. *J. Geotech. Geoenviron. Engng* **124**, No. 3, 254–264.

Clausen, C. J. F., Aas, P. M. & Karlsrud, K. (2005). Bearing capacity of driven piles in sand, the NGI approach. In *Frontiers in offshore geotechnics* (eds S. Gourvenec and M. Cassidy), pp. 547–580. Boca Raton, FL, USA: CRC Press/Balkema.

Dane, J. H. & Hopmans, J. W. (2002). Soil water retention and storage – introduction. In *Methods of soil analysis. Part 4. Physical methods* (eds J. H. Dane and G. C. Topp), Soil Science Society of America Book Series No. 5, pp. 671–674. Madison, WI, USA: Soil Science Society of America.

DiMaggio, J. (1991). *Dynamic pile monitoring and pile load test report*, Demonstration project no. 66,1-165(2). Mobile County, AL, USA: FHWA.

Doherty, P., Kirwan, L., Gavin, K., Igoe, D., Tyrrell, S., Ward, D. & O'Kelly, B. C. (2012). Soil properties at the UCD geotechnical research site at Blessington. *Proceedings of the national bridge and concrete research in Ireland conference*, Dublin, Ireland, pp. 499–504.

Emerson, M., Foray, P., Puech, A. & Palix, E. (2008). A global model for accurately interpreting CPT data in sands from shallow to greater depth. In *Geotechnical and geophysical site characterization* (eds A.-B. Huang and P. W. Mayne), pp. 687–694. London, UK: Taylor & Francis.

Fellenius, B. H. & Altaee, A. (2002). Pile dynamics in geotechnical practice-six case histories. In *Deep foundations 2002, an international perspective on theory, design, construction, and performance* (eds M. W. O'Neill and F. C. Townsend), ASCE Geotechnical Special Publication 116, vol. 1, pp. 619–631. Reston, VA, USA: American Society of Civil Engineers.

Gavin, K. G. & O'Kelly, B. C. (2007). Effect of friction fatigue on pile capacity in dense sand. *J. Geotech. Geoenviron. Engng* **113**, No. 1, 63–71.

Gavin, K. G., Lehane, B. M. & Prieto, C. (2003). The development of skin friction on pipe piles in overconsolidated sand. In *Proceedings, XIII European conference on soil mechanics and geotechnical engineering: geotechnical problems with man-made and man-influenced grounds* (eds I. Vaníček, R. Barvínek, J. Boháč, J. Jettmar, D. Jirásko and J. Salák), vol. 1, pp. 161–166. Prague, Czech Republic: Czech Geotechnical Society CICE.

Gavin, K., Adekunte, A. & O'Kelly, B. (2009). A field investigation of vertical footing response on sand. *Proc. Instn Civ. Engrs – Geotech. Engng* **162**, No. 5, 257–267, https://doi.org/10.1680/geng.2009.162.5.257.

Gavin, K., Igoe, D. & Kirwan, L. (2013). The effect of ageing on the axial capacity of piles in sand. *Proc. Instn Civ. Engrs – Geotech. Engng* **166**, No. 2, 122–130, https://doi.org/10.1680/geng.12.00064.

Gavin, K., Jardine, R. J., Karlsrud, K. & Lehane, B. M. (2015). The effects of pile ageing on the shaft capacity of offshore piles in sand. Keynote paper. In *Frontiers in offshore geotechnics III* (ed. V. Meyer), vol. 1, pp. 129–152. Boca Raton, FL, USA: CRC Press/Balkema.

Ho, Y. K., Jardine, R. J. & Anh-Minh, N. (2011). Large displacement interface shear between steel and granular media. *Géotechnique* **61**, No. 3, 221–234, https://doi.org/10.1680/geot.8.P.086.

Holeyman, A. (2012). Essais de chargement dynamique sur Pieu B-2 de Loon-Plage SOLCYP. *UCL, GeoMEM presentation at the SOLCYP meeting*, Paris, France (in French).

Jardine, R. J. & Chow, F. C. (1996). *New design methods for offshore piles*, MTD Publication 96/103. London, UK: MTD.

Jardine, R. J. & Standing, J. R. (2012). Field axial cyclic loading experiments on piles driven in sand. *Soils Found.* **52**, No. 4, 723–736.

Jardine, R. J., Chow, F. C., Overy, R. F. & Standing, J. R. (2005). *ICP design methods for driven piles in sands and clays*. London, UK: Thomas Telford.

Jardine, R. J., Standing, J. R. & Chow, F. C. (2006). Some observations of the effects of time on the capacity of piles driven in sand. *Géotechnique* **56**, No. 4, 227–244, https://doi.org/10.1680/geot.2006.56.4.227.

Jardine, R. J., Zhu, B. T., Foray, P. & Yang, Z. X. (2013). Interpretation of stress measurements made around closed-ended displacement piles in sand. *Géotechnique* **63**, No. 8, 613–627, https://doi.org/10.1680/geot.9.P.138.

Jardine, R. J., Thomsen, N. V., Mygind, M., Liingaard, M. A. & Thilsted, C. L. (2015). Axial capacity design practice for North European wind-turbine projects. In *Frontiers in offshore geotechnics III* (ed. V. Meyer), vol. 1, pp. 581–586. Boca Raton, FL, USA: CRC Press/Balkema.

Karlsrud, K., Jensen, T. G., Wensaas Lied, E. K., Nowacki, F. & Simonsen, A. S. (2014). Significant ageing effects for axially loaded piles in sand and clay verified by new field load tests. *Proceedings of the offshore technology conference*, Houston, TX, USA, paper OTC-25197-MS, https://doi.org/10.4043/25197-MS.

Kolk, H. J., Baaijens, A. E. & Vergobbi, P. (2005). Results from axial load tests on pipe piles in very dense sands: the EURIPIDES JIP. In *Frontiers in offshore geotechnics* (eds S. Gourvenec and M. Cassidy), pp. 661–667. Boca Raton, FL, USA: CRC Press.

König, F. & Grabe, J. (2006). Time dependent increase of the bearing capacity of displacement piles. In *Proceedings – DFI/EFFC 10th international conference on piling and deep foundations* (eds Amsterdam Conference Organizing Committee, J. Lindberg, M. Bottiau and A. F. Van Tol), pp. 709–717. Hawthorne, NJ, USA: Deep Foundations Institute.

Kuwano, R. (1999). *The stiffness and yielding anisotropy of sand*. PhD thesis, Imperial College, University of London, London, UK.

Lehane, B. (1992). *Experimental investigations of pile behaviour using instrumented field piles*, PhD thesis, Imperial College London, University of London, London, UK.

Lehane, B. M., Jardine, R. J., Bond, A. J. & Frank, R. (1993). Mechanisms of shaft friction from instrumented pile tests. *J. Geotech. Engng* **119**, No. 1, 19–35.

Lehane, B. M., Schneider, J. A. & Xu, X. (2005). The UWA-05 method for prediction of axial capacity of driven piles in sand. In *Frontiers in offshore geotechnics* (eds S. Gourvenec and M. Cassidy), pp. 683–689. Boca Raton, FL, USA: CRC Press/Balkema.

Lehane, B. M., Lim, J. K., Carotenuto, P., Nadim, F., Lacasse, S., Jardine, R. J. & van Dijk, B. F. J. (2017). Characteristics of unified databases for driven piles. In *Offshore site investigation and geotechnics: proceedings of the 8th international conference*, vol. 1, pp. 162–194. London, UK: Society for Underwater Technology.

Lim, J. K. & Lehane, B. M. (2014). Characterisation of the effects of time on the shaft friction of displacement piles in sand. *Géotechnique* **64**, No. 6, 476–485, https://doi.org/10.1680/geot.13.P.220.

NGI (Norwegian Geotechnical Institute) (2009). *Time effects on pile capacity, factual report, test site Larvik*, Report 20061251-00-244-R. Oslo, Norway: Norwegian Geotechnical Institute.

Overy, R. (2007). The use of ICP design methods for the foundations of nine platforms installed in the UK North Sea. In *Proceedings of the 6th international conference of the society for underwater technology, offshore site investigation and geotechnics*, pp. 359–366. London, UK: Society for Underwater Technology.

Prendergast, L. J., Gavin, K. & Doherty, P. (2015). An investigation into the effect of scour on the natural frequency of an offshore wind turbine. *Ocean Engng* **101**, No. 1, 1–11.

Rausche, F., Goble, G. G. & Likins, G. (1985). Dynamic determination of pile capacity. *J. Geotech. Div.* **111**, No. 3, 367–383.

Rimoy, S. (2013). *Ageing and axial cyclic loading studies of displacement piles in sands*. PhD thesis, Imperial College London, University of London, London, UK.

Rimoy, S. P. & Jardine, R. J. (2015). Axial capacity ageing trends of piles driven in silica sands. In *Frontiers in offshore geotechnics III* (ed. V. Meyer), vol. 1, pp. 637–642. Boca Raton, FL, USA: CRC Press/Balkema.

Rimoy, S., Silva, M., Jardine, R. J., Yang, Z. X., Zhu, B. T. & Tsuha, C. H. C. (2015). Field and model investigations into the influence of age on axial capacity of displacement piles in silica sands. *Géotechnique* **65**, No. 7, 576–589, https://doi.org/10.1680/geot.14.P.112.

Samson, L. & Authier, J. (1986). Changes in pile capacity with time: case histories. *Can. Geotech. J.* **23**, No. 1, 174–180.

Schmertmann, J. H. (1991). The mechanical aging of soils. *J. Geotech. Engng* **117**, No. 9, 1288–1330.

Seidel, J. P., Haustorfer, I. J. & Plesiotis, S. (1988). Comparison of dynamic and static testing for piles founded into limestone. In *Proceedings of the 3rd international conference on application of stress-wave theory to piles* (ed. B. H. Fellenius), pp. 717–723. Vancouver, BC, Canada: BiTech Publishers.

Skov, R. & Denver, H. (1988). Time-dependence of bearing capacity of piles. In *Proceedings of the 3rd international conference on application of stress-wave theory to piles* (ed. B. H. Fellenius), pp. 879–888. Vancouver, BC, Canada: BiTech Publishers.

Svinkin, M. R., Morgano, C. M. & Morvant, M. (1994). Pile capacity as a function of time in clayey and sandy soils. In *Proceedings of 5th international conference and exhibition on piling and deep foundations*, pp. 1.11.1–1.11.8. Hawthorne, NJ, USA: Deep Foundations Institute.

Tan, S. L., Cuthbertson, J. & Kimmerling, R. E. (2004). Prediction of pile set-up in non-cohesive soils. In *Current practices and future trends in deep foundations* (eds J. A. DiMaggio and M. H. Hussein). ASCE Geotechnical Special Publication 125, pp. 50–65. Reston, VA, USA: American Society of Civil Engineers.

Tang, W. H., Woodford, D. L. & Pelletier, J. H. (1990). Performance reliability of offshore piles. *Proceedings of the 22nd offshore technology conference*, Houston, TX, USA, paper OTC 6379, pp. 299–308.

Tavenas, F. & Audy, R. (1972). Limitations of the driving formulas for predicting the bearing capacities of piles in sand. *Can. Geotech. J.* **9**, No. 1, 47–62.

Tsuha, C. H. C., Foray, P. Y., Jardine, R. J., Yang, Z. X., Silva, M. & Rimoy, S. (2012). Behaviour of displacement piles in sand under cyclic axial loading. *Soils Found.* **52**, No. 3, 393–410.

White, D. J. & Zhao, Y. (2006). A model-scale investigation into 'set-up' of displacement piles in sand. In *Physical modelling in geotechnics – 6th ICPMG '06* (eds C. W. W. Ng, L. M. Zhang and Y. H. Wang), vol. 2, pp. 889–894. London, UK: Taylor & Francis.

Yang, Z. X., Jardine, R. J., Zhu, B. T., Foray, P. & Tsuha, C. H. C. (2010). Sand grain crushing and interface shearing during displacement pile installation in sand. *Géotechnique* **60**, No. 6, 469–482, https://doi.org/10.1680/geot.2010.60.6.469.

Yang, Z. X., Jardine, R. J., Zhu, B. T. & Rimoy, S. P. (2014). Stresses developed around displacement piles penetration in sand. *J. Geotech. Geoenviron. Engng* **140**, No. 3, 04013027.

Yang, Z. X., Guo, W. B., Jardine, R. J. & Chow, F. (2017). Design method reliability assessment from an extended database of axial load tests on piles driven in sand. *Can. Geotech. J.* **54**, No. 1, 59–74.

York, D. L., Brusey, W. G., Clemente, E. M. & Law, S. K. (1994). Set-up and relaxation in glacial sand. *J. Geotech. Engng* **120**, No. 9, 1498–1513.

Zai, J. (1988). Pile dynamic testing experience in Shanghai. In *Proceedings of the 3rd international conference on application of stress-wave theory to piles* (ed. B. H. Fellenius), pp. 781–792. Vancouver, BC, Canada: BiTech Publishers.

Zdravković, L., Jardine, R. J., Taborda, D. M. G., Burd, H. J., Byrne, K., Gavin, K., Houlsby, G. T., Igoe, D., Liu, T., Martin, C. M., McAdam, R. A., Muir-Wood, A., Potts, D. M., Skov Gretlund, J. & Ushev, E. (2019). Ground characterisation for PISA pile testing and analysis. *Géotechnique*, https://doi.org/10.1680/jgeot.18.PISA.001.

Zhang, C., Yang, Z. X., Nguyen, G. D., Jardine, R. J. & Einav, I. (2014). Theoretical breakage mechanics and experimental assessment of stresses surrounding piles penetrating into dense silica sand. *Géotechnique Lett.* **4**, No. 1, 11–16, https://doi.org/10.1680/geolett.13.00075.